Supporting Information

Engineering of halohydrin dehalogenase for the regio- and stereoselective synthesis of (*S*)-4-aryl-2-oxazolidinones

Authors: Jinsong Song[a,b], Chuanhua Zhou[c],Xi Chen[b], Feng Xue[a*], Qiaqing Wu[b*], and Dunming Zhu[b]

[a] School of Food Science and Pharmaceutical Engineering, Nanjing Normal University, NO. 1, Wenyuan Road, Nanjing 210023, People's Republic of China

[b] National Engineering Laboratory for Industrial Enzymes and Tianjin Engineering Research Center of Biocatalytic Technology, Tianjin Institute of Industrial Biotechnology, Chinese Academy of Sciences, 32 Xi Qi Dao, Tianjin Airport Economic Area, Tianjin 300308, China

[c] Tianjin Changlu Haijing Group Co., Ltd. No. 1088, Yingkou Road, Tanggu, Binhai New Area, Tianjin, 300450, China

***Corresponding author:**

Feng Xue

E-mail address: xuef2020@njnu.edu.cn;

Tel.:+86-25-58889625;

Fax: +86-25-58889625

Qiaqing Wu

E-mail address: wu_qq@tib.cas.cn;

Tel.:+86-022-84861963;

Fax: +86-022-84861996

Preparation of chemicals

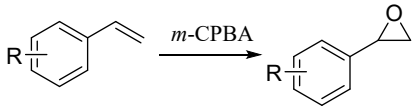

Sheme 1. Methods for the synthesis of **1c-1e, 1g**, **1h** and **1j**.

The substrates styrene oxide derivatives **1c-1e, 1g**, **1h** and **1j** were prepared from commercially available substituted styrene via reaction with *meta*-chloroperoxybenzoic acid (*m*-CPBA)[1].

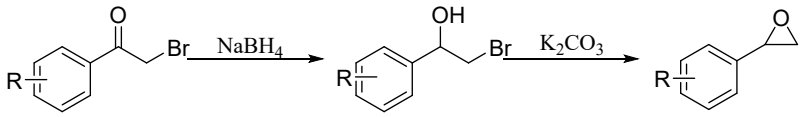

Sheme 2. Methods for the synthesis of **1b**, **1f**, **1i**, **1k** and **1l**.

The substrates **1b**, **1f**, **1i**, **1k** and **1l** were prepared from the corresponding substituted 2-bromo-1-phenylethan-1-one by two-step reactions[2].

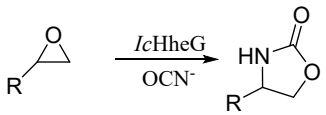

Sheme 3. Methods for the synthesis of (*R*/*S*)**-2a-2l**.

Racemic **2a-2l** were synthesized from epoxides **1a-1l** using *Ic*HheG. The reaction system consisted of 40 mL Tris-SO_4 buffer (50 mM, pH 7.5), 50 g/L *E. coli* (*Ic*HheG), 50 mM substrate, 75 mM NaOCN and 2.5% DMSO as a co-solvent. The bacteria were re-suspended, mixed and reacted at 200 rpm at 30 ℃ for 6 h, and the reaction was terminated by adding the same amount of petroleum ether (3×40 mL). The remaining aqueous phase was extracted three times with the same volume of ethyl acetate. After the organic phase was combined, it was cleaned three times with saturated salt water and deionized water respectively. The organic phase was dried by anhydrous Na_2SO_4, and then concentrated to obtain oxazolidinone. The crude products were purified by preparative TLC with the spreading solvent (n-hexane/ethyl acetate 1:1). These purified racemic compounds were identified by NMR analysis.

General procedure for the Synthesis of chiral oxazolidinones by enzymatic kinetic resolution

The reaction system consisted of 40 mL Tris-SO_4 buffer (50 mM, pH 7.5), 50 g/L *E. coli* (*Ic*HheG-I104F/N196W), 15-50 mM substrate, 1.5 eq NaOCN and 2.5% DMSO as a co-solvent. The wet cells with HHDHs were re-suspended, mixed and reacted at 200 rpm at 30 ℃ for 6 h, and the reaction was extracted by petroleum ether (3×40 mL). Combine organic phase and dry with anhydrous sodium sulfate. The chiral epoxide (*S*)**-1a-1l** was obtained by evaporating under reduced pressure and confirmed by GC analysis.

The remaining aqueous phase was extracted three times with the same volume of ethyl acetate. The combined organic phase was washed with saturated salt water 3 times and deionized water 3 times. The organic layer was dried with anhydrous sodium sulfate and concentrated under reduced pressure to obtain chiral oxazolidinones (*S*)**-2a-2l**. The crude products were purified by preparative TLC with the spreading solvent (n-hexane/ethyl acetate 1:1). Chiral oxazolidinones were identified by NMR and HPLC analysis.

(*S*)-4-phenyloxazolidin-2-one (2a)

White solid, 136 mg, 42% yield, 96% *ee*; Chiralpak IC, *n*-hexane/*i*-PrOH=80/20, flow rate 1 mL/min, λ=210 nm, t(*S*)**-2a**=27.3 min, t(*R*)**-2a** =40.5 min.^{1}H NMR (400MHz, $CDCl_3$) δ = 7.45 - 7.22 (m, 5H), 6.42 (br. s., 1H), 4.95 (t, *J* = 7.7 Hz, 1H), 4.72 (t, *J* = 8.6 Hz, 1H), 4.16 (t, *J* = 7.7 Hz, 1H). ^{13}C NMR (100 MHz, $CDCl_3$) δ 159.93, 139.46, 129.13, 128.73, 125.97, 72.49, 56.32.

(*S*)-4-(2-tolyl)oxazolidin-2-one (2b)

White solid, 99 mg, 28% yield, 81% *ee*; Chiralpak OD-H, *n*-hexane/*i*-PrOH = 90/10, flow rate 0.6 mL/min, λ = 220 nm, t(*S*)**-2b**= 67.2 min, t(*R*)**-2b** = 44.5 min. ^{1}H NMR (400MHz, $CDCl_3$) δ = 7.49 - 7.39 (m, 1H), 7.34 - 7.11 (m, 3H), 6.27 - 6.09 (m, 1H), 5.27 - 5.17 (m, 1H), 4.78 (t, *J* = 8.6 Hz, 1H), 4.10 (t, *J* = 7.7 Hz, 1H), 2.30 (s, 3H). ^{13}C NMR (100 MHz, $CDCl_3$) δ 159.96, 137.46, 134.56, 130.87, 128.28, 126.92, 124.67, 71.55, 53.11, 19.01.

(*S*)-4-(3-tolyl)oxazolidin-2-one (2c)

White solid, 128 mg, 36% yield, 58% *ee*; Chiralpak OD-H, *n*-hexane/*i*-PrOH = 95/5, flow rate 0.6 mL/min, λ = 220 nm, t(*S*)**-2c**= 89.9 min, t(*R*)**-2c**= 86.4 min. ^{1}H NMR (400MHz, $CDCl_3$) δ = 7.27 (d, *J* = 7.8 Hz, 1H), 7.21 - 7.06 (m, 3H), 5.99 - 5.82 (m, 1H), 4.96 - 4.86 (m, 1H), 4.72 (t, *J* = 8.7 Hz, 1H), 4.18 (dd, *J* = 7.2, 8.2 Hz, 1H), 2.37 (s, 3H). ^{13}C NMR (100 MHz, $CDCl_3$) δ 159.63, 139.39, 139.06, 129.55, 129.06, 126.62, 123.09, 72.54, 56.30, 21.37.

(*S*)-4-(4-tolyl)oxazolidin-2-one (2d)

White solid, 188 mg, 53% yield, 66% *ee*; Chiralpak OD-H, *n*-hexane/*i*-PrOH = 90/10, flow rate 0.6 mL/min, λ = 220 nm, t(*S*)**-2d**= 60.1 min, t(*R*)**-2d**= 46.4 min. ^{1}H NMR (400MHz, $CDCl_3$) δ = 7.21 (d, *J* = 1.7 Hz, 4H), 6.11 - 6.03 (m, 1H), 4.96 - 4.85 (m, 1H), 4.70 (s, 1H), 4.16 (d, *J* = 7.3 Hz, 1H), 2.35 (s, 3H). ^{13}C NMR (100 MHz, $CDCl_3$) δ 159.75, 138.66, 136.41, 129.78, 125.95, 72.61, 56.14, 21.09.

(*S*)-4-(2-fluorophenyl)oxazolidin-2-one (2e)

White solid, 46 mg, 47% yield, 97% *ee*; Chiralpak OD-H, *n*-hexane/*i*-PrOH = 90/10, flow rate 0.6 mL/min, λ = 220 nm, t(*S*)**-2e**= 36.7 min, t(*R*)**-2e**= 47.5 min. ^{1}H NMR (400MHz, $CDCl_3$) δ = 7.44 - 7.33

(m, 1H), 7.26 (s, 1H), 7.13 (d, *J* = 7.8 Hz, 1H), 7.07 (d, *J* = 8.8 Hz, 2H), 6.04 - 5.87 (m, 1H), 4.96 (d, *J* = 7.6 Hz, 1H), 4.75 (t, *J* = 8.7 Hz, 1H), 4.17 (s, 1H). ^{13}C NMR (100 MHz, CDCl3) δ 164.41, 161.95 , 159.43 , 142.04, 141.97, 130.99, 130.92, 121.60, 115.98, 115.77, 113.16, 112.94, 72.23, 55.87.

(*S*)-4-(4-fluorophenyl)oxazolidin-2-one (2f)

White solid, 161 mg, 45% yield, 99% *ee*; Chiralpak OD-H, *n*-hexane/*i*-PrOH = 90/10, flow rate 0.6 mL/min, λ = 220 nm, t(*S*)-**2f**= 39.4 min, t(*R*)-**2f**= 45.7 min. ^{1}H NMR (400MHz, $CDCl_3$) δ = 7.38 - 7.22 (m, 2H), 7.10 (t, *J* = 8.4 Hz, 2H), 5.99 (br. s., 1H), 4.96 (t, *J* = 7.7 Hz, 1H), 4.73 (t, *J* = 8.7 Hz, 1H), 4.22 - 4.08 (m, 1H). ^{13}C NMR (100 MHz, CDCl3) δ 164.09, 161.62, 159.54, 135.18, 135.18, 127.87, 127.79, 116.30, 116.09, 72.50, 55.76.

(*S*)-4-(2-chlorophenyl)oxazolidin-2-one (2g)

White solid, 56 mg, 14% yield, 98% *ee*; Chiralpak OD-H, *n*-hexane/*i*-PrOH = 90/10, flow rate 0.6 mL/min, λ = 220 nm, t(*S*)-**2g**= 42.5 min, t(*R*)-**2g**= 60.4 min. ^{1}H NMR (400MHz, $CDCl_3$) δ = 7.50 (s, 1H), 7.45 - 7.25 (m, 3H), 6.52 - 6.37 (m, 1H), 5.38 (br. s., 1H), 4.90 (s, 1H), 4.15 (dd, *J* = 6.4, 8.6 Hz, 1H). ^{13}C NMR (100 MHz, $CDCl_3$) δ 159.99, 137.25, 132.05, 129.90, 127.63, 126.12, 71.29, 53.22.

(*S*)-4-(3-chlorophenyl)oxazolidin-2-one (2h)

White solid, 169 mg, 43% yield, 98% ee; Chiralpak OD-H, *n*-hexane/*i*-PrOH = 95/5, flow rate 0.6 mL/min, λ = 220 nm, t(*S*)-**2h**= 104.8 min, t(*R*)-**2h**= 120.7 min. ^{1}H NMR (400MHz, $CDCl_3$) δ = 7.42 - 7.20 (m, 4H), 5.94 (br. s., 1H), 5.60 (t, *J* = 8.1 Hz, 1H), 4.01 (t, *J* = 8.7 Hz, 1H), 3.52 (t, *J* = 8.1 Hz, 1H). ^{13}C NMR (100 MHz, $CDCl_3$) δ 159.40, 140.44, 134.92, 130.27, 129.07, 125.76, 123.65, 48.13.

(*S*)-4-(4-chlorophenyl)oxazolidin-2-one (2i)

White solid, 162 mg, 41% yield, 98% *ee*; Chiralpak OD-H, *n*-hexane/*i*-PrOH = 90/10, flow rate 0.6 mL/min, λ = 220 nm, t(*S*)-**2i**= 53.2 min, t(*R*)-**2i**= 58.2 min. ^{1}H NMR (400MHz, $CDCl_3$) δ = 7.38 (d, *J* = 8.3 Hz, 2H), 7.28 (d, *J* = 8.6 Hz, 2H), 6.24 (br. s., 1H), 4.95 (s, 1H), 4.79 - 4.68 (m, 1H), 4.20 - 4.09 (m, 1H). ^{13}C NMR (100 MHz, $CDCl_3$) δ 159.68, 137.94, 134.69, 129.39, 127.40, 72.33, 55.76.

(*S*)-4-(3-bromophenyl)oxazolidin-2-one (2j)

White solid, 115 mg, 24% yield, 98% *ee*; Chiralpak OD-H, *n*-hexane/*i*-PrOH = 90/10, flow rate 0.6 mL/min, λ = 220 nm, t(*S*)-**2j**= 64.1min, t(*R*)-**2j**= 59.6 min. ^{1}H NMR (400MHz, $CDCl_3$) δ = 7.48 (s, 2H), 7.27 (d, *J* = 4.4 Hz, 2H), 6.65 - 6.51 (m, 1H), 4.93 (t, *J* = 7.8 Hz, 1H), 4.72 (t, *J* = 8.8 Hz, 1H), 4.15 (dd, *J* = 7.1, 8.3 Hz, 1H). ^{13}C NMR (100 MHz, $CDCl_3$) δ 159.83, 141.84, 131.86, 130.76, 129.10, 124.59, 123.17, 123.15, 72.19, 55.73.

(*S*)-4-(4-bromophenyl)oxazolidin-2-one (2k)

White solid, 192 mg, 40% yield, 98% *ee*; Chiralpak OD-H, *n*-hexane/*i*-PrOH = 90/10, flow rate 0.6 mL/min, λ = 220 nm, t(*S*)-**2k**= 61.1min, t(*R*)-**2k**= 69.4 min. ^{1}H NMR (400MHz, $CDCl_3$) δ = 7.53 (d, *J* = 8.1 Hz, 2H), 7.22 (d, *J* = 8.1 Hz, 2H), 6.29 (br. s., 1H), 4.93 (t, *J* = 7.8 Hz, 1H), 4.73 (t, *J* = 8.7 Hz, 1H), 4.13 (t, *J* = 7.7 Hz, 1H). ^{13}C NMR (100 MHz, $CDCl_3$) δ 159.61, 138.45, 132.36, 127.71, 122.81, 72.25, 55.82.

(*S*)-4-(3,4-dichlorophenyl)oxazolidin-2-one (2l)

White solid, 111 mg, 24% yield, 97% *ee*; Chiralpak OD-H, *n*-hexane/*i*-PrOH = 80/20, flow rate 0.4 mL/min, λ = 220 nm, t(*S*)-**2l**= 36.9min, t(*R*)-**2l**= 44.8 min. ^{1}H NMR (400MHz, $CDCl_3$) δ = 7.53 - 7.41 (m, 2H), 7.19 (dd, *J* = 1.5, 8.1 Hz, 1H), 6.69 (br. s., 1H), 4.94 (t, *J* = 7.7 Hz, 1H), 4.74 (t, *J* = 8.8 Hz, 1H), 4.13 (dd, *J* = 6.8, 8.3 Hz, 1H). ^{13}C NMR (100 MHz, $CDCl_3$) δ 159.78, 137.74, 133.39, 132.94, 131.23, 128.09, 125.24, 72.05, 55.35.

Table S1 Oligonucleotide sequences used in this study.

Target sites	Oligonucleotide sequences
Y18A	GCAACCGGTGCAGTTGGTCCGGCAC
18R	CCAGGCATGCACTATCCAGGCGACC
V100A	GTGCATGCCTGGCAACCGGCCTGAT
T101A	GCATGCCTGGTGGCAGGCCTGATTG
L103A	GCCTGGTGACCGGCGCAATTGTTAC
I104A	GGTGACCGGCCTGGCAGTTACCGGCAAA
100-104R	CCACTGCGCGAACAATACCATTGGC
T151A	GTGTGTTGTGTTTGCAAGTGCCACCGG
T154A	GTTTACCAGTGCCGCAGGCGGTCGTC
151-154R	GGAACCTGGGCTTCAATCATTGCGC
T195A	GCAATTGGTGCAAATTATATGGATTTCCCG
N196A	GCAATTGGTACCGCATATATGGATTTCCCG
Y197A	GCAATTGGTACCAATGCAATGGATTTCCCG
F200A	CCAATTATATGGATGCACCGGGCTTTCT
195-200R	GAAAACGATTACTACCATCCAGCAGGCC
L103G/I104A	GGTGACCGGCGGTGCAGTTACCGGCAAA
L103G/I104-R	CCACTGCGCGAACAATACCATTGGC

The above primers were used for site-specific mutagenesis. The amino acid at each site mutates into 19 other amino acids, and the corresponding codon preferred by *E. coli* was selected to replace the red-marked codon.

Table S2 Summary of HHDHs catalyzed SO for the synthesis of oxazolidinone from the recent literature[3,4].

Entry[a]	HHDH	Substrate	Relative activity[b] [%]	Ratio **2a**:**3a**	**2a** *ee*[c] [%]
1[3]	Control[d]	SO	<1	ND	ND
2[3]	*Cs*HheA	SO	31	26:74	32 (*R*)
3[3]	*Cs*HheB	SO	66	12:88	79 (*R*)
4[3]	*Gb*HheB	SO	49	57:43	69 (*R*)
5[3]	*Ar*HheC	SO	94	41:59	72 (*S*)
6[3]	*Ss*HheD	SO	80	95:5	38 (*R*)
7[3]	*Eb*HheD	SO	72	96:4	42 (*R*)
8[3]	*Ni*HheG	SO	35	97:3	65 (*R*)
9[3]	*Ac*HheG	SO	57	99:1	34 (*S*)
10[3]	*Ab*HheG	SO	135	98:2	30 (*R*)
11[3]	*Ic*HheG	SO	100	91:9	31 (*S*)
12[4]	*Ic*HheG[ef]	*R*-SO	ND	ND	>99 (*S*)
13[4]	*Ic*HheG[ef]	*S*-SO	ND	ND	>99 (*R*)

[a] Reaction conditions: 1 mL Tris-SO_4 buffer (50 mM, pH 7.5), 1a (10 mM), 1% DMSO, NaOCN (15 mM), wet cells of *E. coli* (HHDH) (25 g/L), 30 °C. [b] The amount of product performed at 2.5 h was used to indicate the activity. As the positive control, the activity of *Ic*HheG was defined as 100% and the selectivity data are from the references. [c] Absolute configurations were determined by comparison with references. [d] Host *E. coli* BL21(DE3) cells without the HHDH gene were used. [e] Configurations were defined using commercial enantiopure (*R*)-2a and (*S*)-2a. The *ee* values were determined by chiral HPLC. [f] Reaction conditions: PB buffer (50 mM, pH 7.5) 30 mL, cell density 15 g cdw/L, epoxides conc. 15 mM, NaOCN conc. 45 mM, reaction temperature 30 °C, reaction time 12 h. ND=not determined. All reactions were performed in triplicate.

Table S3 Alanine-scanning mutagenesis of wild-type *Ic*HheG with **1a**.[a]

Mutant	Relative activity (%)	**2a:3a**	**2a** *ee*(%)
WT	100[b]	93:7	33 (*S*)
Y18A	0	-	-
L103A	133	99:1	50 (*S*)
I104A	0	-	-
T151A	0	-	-
A153L	0	-	-
T154A	0	-	-
T195A	6	ND[c]	ND
N196A	43	95:5	34 (*R*)
Y197A	0	-	-
F200A	0	-	-

[a] Reactions were carried out in 1 mL Tris-SO_4 buffer (50 mM, pH 7.5) containing *E. coli* (HHDH) wet cells (50 g/L), 1% v/v DMSO, **1a** (10 mM) and NaOCN (15 mM) at 30 °C, 200 rpm for 3 h. [b]The activity of wild type *Ic*HheG towards **1a** was defined as 100%. [c] ND means not detected.

Table S4 Relative activity, regio- and stereoselectivity of mutants towards **1a** by using resting cells.[a]

Mutant	Relative activity (%)	Ratio **2a**:**3a**	**2a** *ee*(%)
Y18H	82	>99:1	82 (*S*)
Y18F	122	>99:1	65 (*S*)
L103G	99	>99:1	83 (*S*)
L103Q	130	>99:1	39 (*S*)
L103E	121	>99:1	39 (*S*)
L103T	155	98:2	32 (*S*)
L103W	150	96:4	48 (*S*)
L103F	67	98:2	71 (*S*)
L103V	166	97:3	24 (*S*)
L103Y	148	99:1	40 (*S*)
L103D	155	98:2	34 (*S*)
L103R	127	>99:1	51 (*S*)
L103N	129	98:2	56 (*S*)
L103M	150	98:2	42 (*S*)
L103K	137	97:3	50 (*S*)
L103I	125	>99:1	34 (*S*)
L103S	133	>99:1	49 (*S*)
L103H	134	>99:1	44 (*S*)
I104N	70	99:1	95 (*S*)
I104Y	102	99:1	82 (*S*)
I104T	28	98:2	84 (*S*)
I104H	105	97:3	75 (*S*)
I104L	102	99:1	69 (*S*)
I104C	100	99:1	65 (*S*)
I104Q	70	99:1	83 (*S*)
I104M	121	>99:1	50 (*S*)
I104S	44	96:4	91 (*S*)
I104E	35	99:1	83(*S*)
I104F	80	97:3	81 (*S*)
N196G	102	95:5	30 (*R*)
N196C	126	99:1	36 (*S*)
N196Y	7	ND	ND
N196Q	2	ND	ND
N196W	82	>99:1	75 (*S*)
N196L	116	98:2	22 (*S*)
N196H	67	>99:1	60 (*S*)
N196F	48	>99:1	67 (*S*)
N196M	15	>99:1	22 (*S*)
N196S	4	ND	ND

[a] Reactions were carried out in 1 mL Tris-SO_4 buffer (50 mM, pH 7.5) containing *E. coli* (HHDH) wet cells (50 g/L), 1% v/v DMSO, **1a** (10 mM) and NaOCN (15 mM) at 30 °C, 200 rpm for 3 h.

Table S5 Relative activity, regio- and stereoselectivity of multisite variants toward styrene oxide.[a]

*Ic*HheG mutants	Relative activity(%)	**2a**:**3a**	**2a** *ee* (%)
WT	100	93:7	33 (*S*)
Y18F/L103K	99	>99:1	73 (*S*)
Y18F/L103F	98	>99:1	60 (*S*)
Y18F/L103H	106	>99:1	64 (*S*)
Y18F/L103D	109	>99:1	64 (*S*)
Y18F/L103R	82	>99:1	76 (*S*)
Y18F/L103E	112	>99:1	52 (*S*)
Y18F/L103M	97	>99:1	72 (*S*)
Y18F/L103Q	96	>99:1	72 (*S*)
Y18F/L103N	100	>99:1	61 (*S*)
Y18F/L103C	101	>99:1	72 (*S*)
Y18F/L103G	97	>99:1	75 (*S*)
Y18W/N196W	22	99:1	95 (*S*)
Y18H/N196W	34	98:2	32 (*R*)
Y18M/N196W	4	ND	ND
Y18N/N196W	26	97:3	96 (*S*)
Y18H/N196F	23	96:4	12 (*S*)
Y18H/N196L	13	94:6	15 (*S*)
Y18H/N196M	55	>99:1	37 (*S*)
Y18H/N196G	31	95:5	67 (*R*)
L103G/I104N	32	95:5	91 (*S*)
L103G/I104T	61	95:5	88 (*S*)
L103G/I104F	76	98:2	95 (*S*)
L103G/I104Y	85	98:2	77 (*S*)
L103G/I104M	125	96:4	62 (*S*)
L103G/I104R	50	93:7	95 (*S*)
L103G/I104E	25	90:10	87 (*S*)
L103G/I104G	23	93:7	89 (*S*)
L103G/I104K	35	92:8	89 (*S*)
L103G/T195S	42	85:15	71 (*S*)
L103G/T195M	30	99:1	94 (*S*)
L103G/T195W	77	98:2	80 (*S*)
L103G/N196C	204	98:2	49 (*S*)
L103G/N196F	54	>99:1	76 (*S*)
L103G/N196H	98	>99:1	79 (*S*)
L103G/N196L	150	97:3	49 (*S*)
L103G/N196M	165	97:3	27 (*S*)
L103G/N196Q	42	95:5	89 (*S*)
L103G/N196Y	28	91:9	79 (*S*)
L103C/N196W	136	97:3	79 (*S*)
L103D/N196W	187	93:7	66 (*S*)
L103E/N196W	154	97:3	57 (*S*)

L103H/N196W	145	93:7	73 (*S*)
L103M/N196W	135	96:4	79 (*S*)
L103N/N196W	143	>99:1	76 (*S*)
L103Q/N196W	156	97:3	76 (*S*)
L103S/N196W	149	>99:1	77 (*S*)
L103T/N196W	146	>99:1	70 (*S*)
L103Y/N196W	112	>99:1	82 (*S*)
L103A/N196W	188	97:3	57 (*S*)
L103G/N196W	84	98:2	90 (*S*)
I104H/N196W	50	95:5	97 (*S*)
I104Y/N196W	72	97:3	96 (*S*)
I104W/N196W	87	99:1	91 (*S*)
I104V/N196W	92	99:1	85 (*S*)
I104F/N196W	73	>99:1	98 (*S*)
I104C/N196W	43	99:1	98 (*S*)
I104G/N196W	56	98:2	95 (*S*)

[a] Reactions were carried out in 1 mL Tris-SO_4 buffer (50 mM, pH 7.5) containing *E. coli* (HHDH) wet cells (50 g/L), 1% v/v DMSO, **1a** (10 mM) and NaOCN (15 mM) at 30 °C, 200 rpm for 3 h.

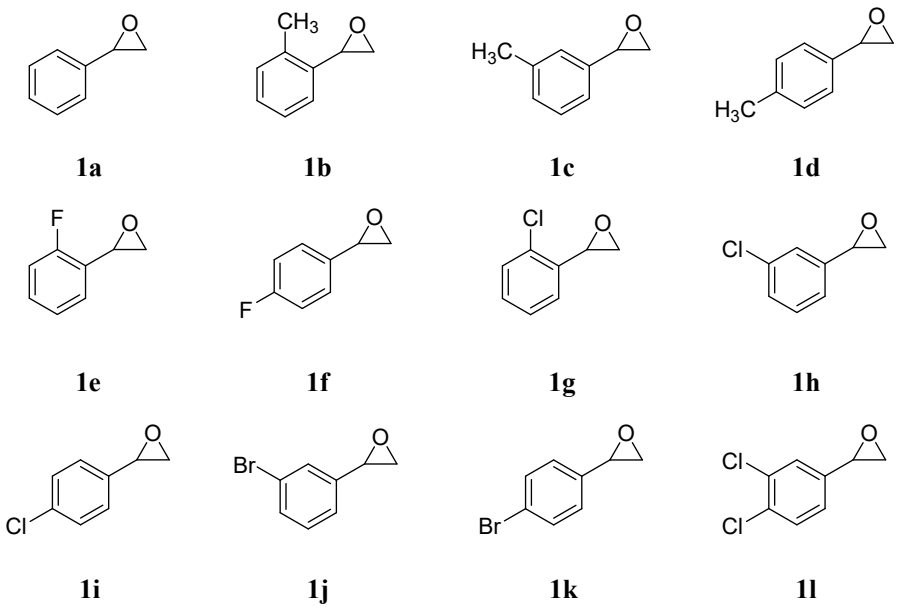

Fig. S1 Epoxide used as substrates in this study.

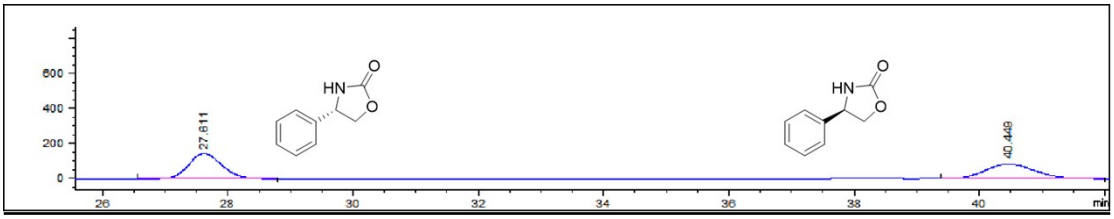

ID#	Ret.Time	Area	Height	Area %
1	27.611	5253.9	143.7	53.827
2	40.449	4506.8	83.9	46.173

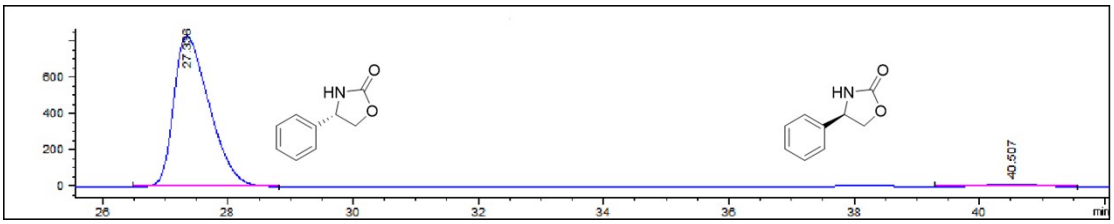

ID#	Ret.Time	Area	Height	Area %
1	27.336	32612.6	830.7	97.891
2	40.507	702.7	14.1	2.109

We established a large-scale biological reaction with epoxyethane **1a** (1.2g) as the substrate. The reaction was continued for 6 hours with a substrate concentration of 50mM. After treatment, the final yield was 38%(0.61g).

The *ee* was determined by chiral HPLC (Chiralpak IC, *n*-hexane/*i*-PrOH=80/20, flow rate 1 mL/min, λ=210 nm, t(*S*)-**2a**=27.3 min, t(*R*)-**2a** =40.5 min).

Fig. S2 HPLC chromatograms of *rac*-**2a** synthesized by *Ic*HheG, (*S*)-**2a** synthesized by mutant I104F/N196W.

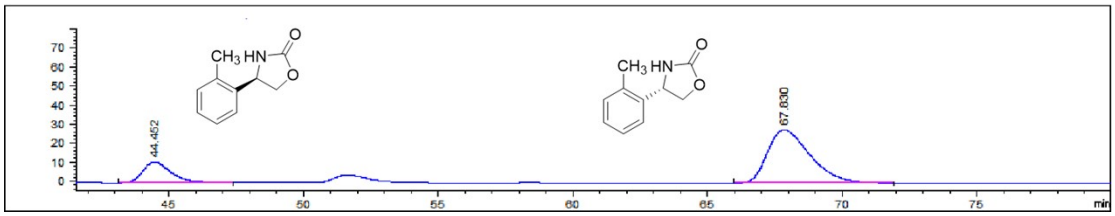

ID#	Ret.Time	Area	Height	Area %
1	44.452	797.7	10.9	20.492
2	67.83	3095.3	28	79.508

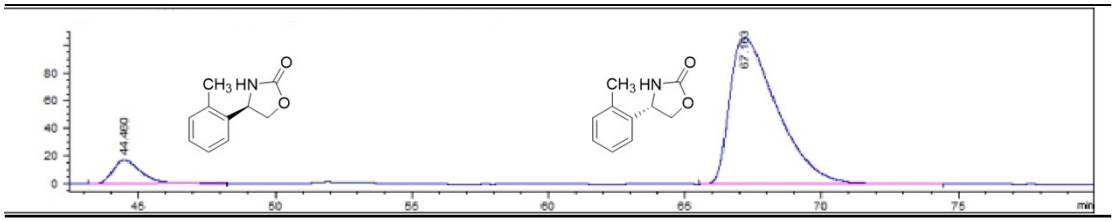

ID#	Ret.Time	Area	Height	Area %
1	44.46	1309.9	17.2	9.251
2	67.163	12849.6	106.2	90.749

The *ee* was determined by chiral HPLC (Chiralpak OD-H, *n*-hexane/*i*-PrOH = 90/10, flow rate 0.6 mL/min, λ = 220 nm, t(*S*)-**2b**= 67.2 min, t(*R*)-**2b** = 44.5 min).

Fig. S3 HPLC chromatograms of *rac*-**2b** synthesized by *Ic*HheG, (*S*)-**2b** synthesized by mutant I104F/N196W.

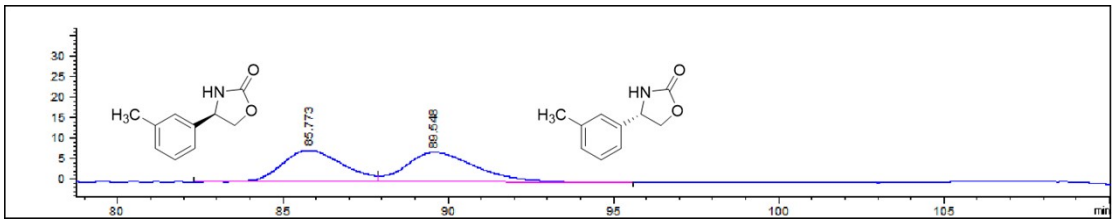

ID#	Ret.Time	Area	Height	Area %
1	85.773	1001.5	7.7	48.024
2	89.548	1083.9	7.3	51.976

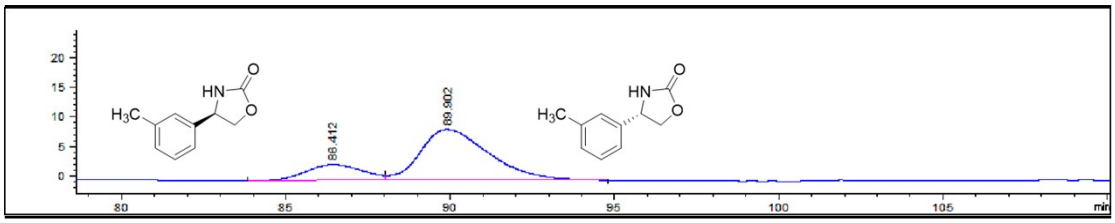

ID#	Ret.Time	Area	Height	Area %
1	86.413	343.7	2.8	20.985
2	89.901	1294.3	8.7	79.015

The *ee* was determined by chiral HPLC (Chiralpak OD-H, *n*-hexane/*i*-PrOH = 95/5, flow rate 0.6 mL/min, λ = 220 nm, t(*S*)-**2c**= 89.9 min, t(*R*)-**2c**= 86.4 min).

Fig. S4 HPLC chromatograms of *rac*-**2c** synthesized by *Ic*HheG, (*S*)-**2c** synthesized by mutant I104F/N196W.

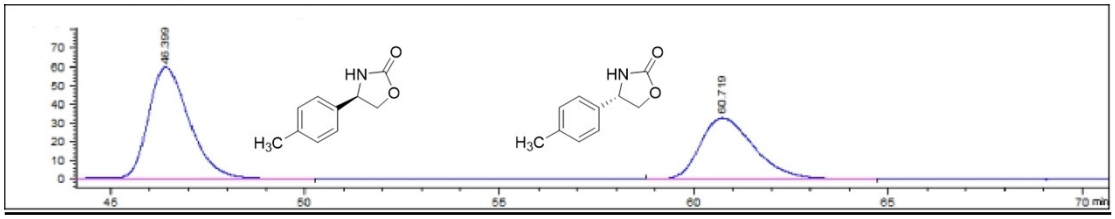

ID#	Ret.Time	Area	Height	Area %
1	46.399	4411.8	59.9	58.229
2	60.719	3164.8	32.8	41.771

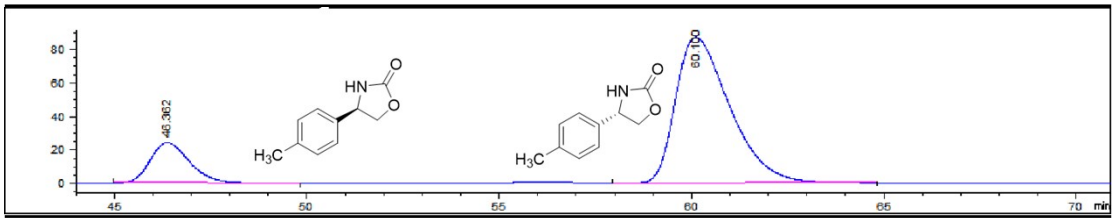

ID#	Ret.Time	Area	Height	Area %
1	46.362	1745.2	24.3	16.895
2	60.1	8584.5	87.3	83.105

The *ee* was determined by chiral HPLC (Chiralpak OD-H, *n*-hexane/*i*-PrOH = 90/10, flow rate 0.6 mL/min, λ = 220 nm, t(*S*)-**2d**= 60.1 min, t(*R*)-**2d**= 46.4 min).

Fig. S5 HPLC chromatograms of *rac*-**2d** synthesized by *Ic*HheG, (*S*)-**2d** synthesized by mutant I104F/N196W.

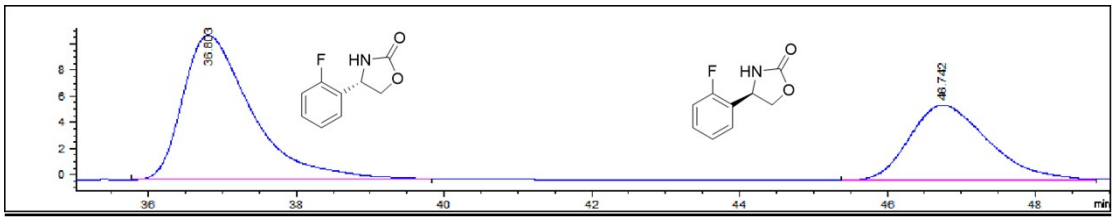

ID#	Ret.Time	Area	Height	Area %
1	36.803	716.9	11.1	62.358
2	46.742	432.7	5.8	37.642

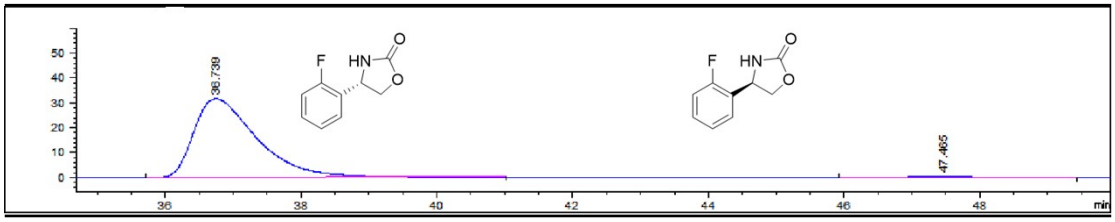

ID#	Ret.Time	Area	Height	Area %
1	36.739	2085.7	31.8	98.698
2	47.457	27.5	3.8E-1	1.302

The *ee* was determined by chiral HPLC (Chiralpak OD-H, *n*-hexane/*i*-PrOH = 90/10, flow rate 0.6 mL/min, λ = 220 nm, t(*S*)-**2e**= 36.7 min, t(*R*)-**2e**= 47.5 min).

Fig. S6 HPLC chromatograms of *rac*-**2e** synthesized by *Ic*HheG, (*S*)-**2e** synthesized by mutant I104F/N196W.

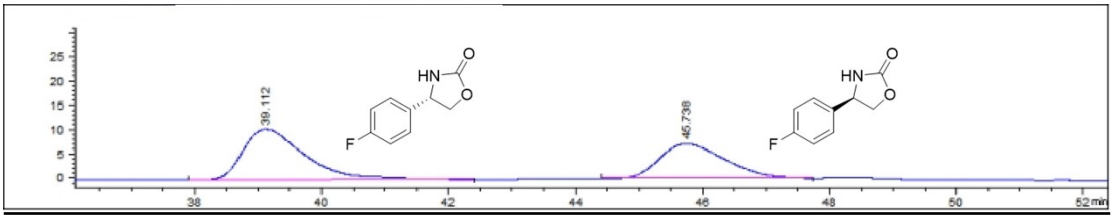

ID#	Ret.Time	Area	Height	Area %
1	39.112	718.1	10.5	58.221
2	45.738	515.3	7.2	41.779

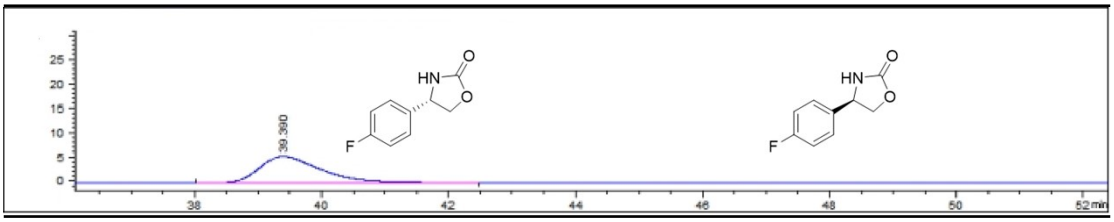

ID#	Ret.Time	Area	Height	Area %
1	39.39	376.9	5.5	100

The *ee* was determined by chiral HPLC (Chiralpak OD-H, *n*-hexane/*i*-PrOH = 90/10, flow rate 0.6 mL/min, λ = 220 nm, t(*S*)-**2f**= 39.4 min, t(*R*)-**2f**= 45.7 min).

Fig. S7 HPLC chromatograms of *rac*-**2f** synthesized by *Ic*HheG, (*S*)-**2f** synthesized by mutant I104F/N196W.

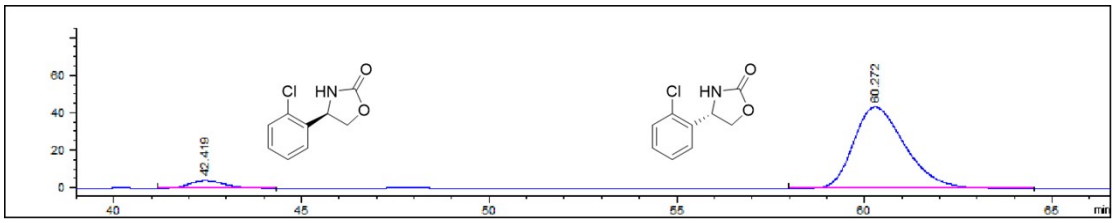

ID#	Ret.Time	Area	Height	Area %
1	42.419	270.2	4	6.074
2	60.272	4178.8	43.5	93.926

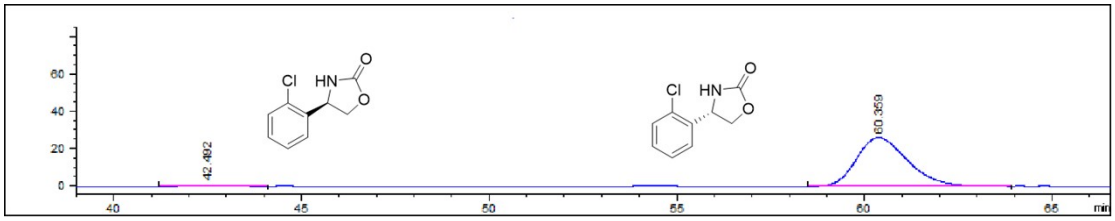

ID#	Ret.Time	Area	Height	Area %
1	42.492	29.5	4.4E-1	1.183
2	60.359	2462.7	26.1	98.817

The *ee* was determined by chiral HPLC (Chiralpak OD-H, *n*-hexane/*i*-PrOH = 90/10, flow rate 0.6 mL/min, λ = 220 nm, t(*S*)-**2g**= 42.5 min, t(*R*)-**2g**= 60.4 min).

Fig. S8 HPLC chromatograms of *rac*-**2g** synthesized by *Ic*HheG, (*S*)-**2g** synthesized by mutant I104F/N196W.

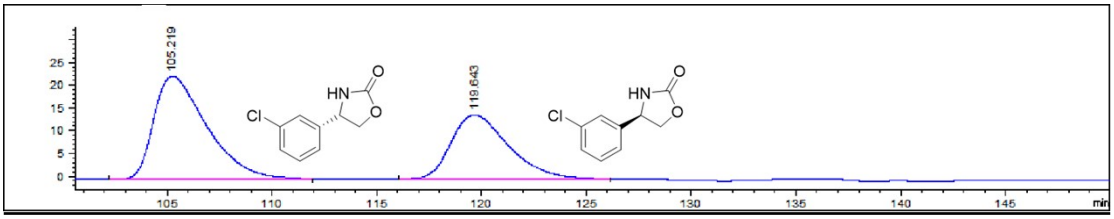

ID#	Ret.Time	Area	Height	Area %
1	105.219	3992.6	22.5	59.527
2	119.643	2714.6	14.2	40.473

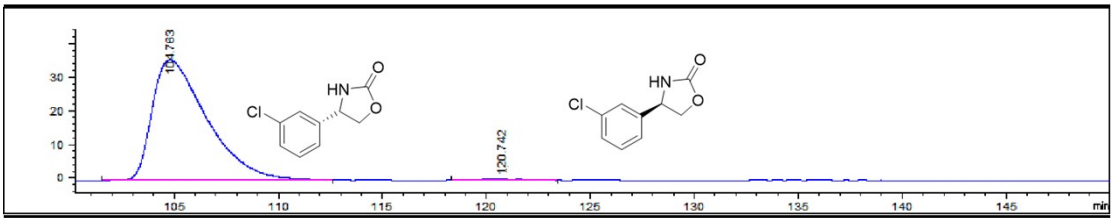

ID#	Ret.Time	Area	Height	Area %
1	104.763	6584.1	36	98.821
2	120.742	78.6	4.8E-1	1.179

The *ee* was determined by chiral HPLC (Chiralpak OD-H, *n*-hexane/*i*-PrOH = 95/5, flow rate 0.6 mL/min, λ = 220 nm, t(*S*)-**2h**= 104.8 min, t(*R*)-**2h**= 120.7 min).

Fig. S9 HPLC chromatograms of *rac*-**2h** synthesized by *Ic*HheG, (*S*)-**2h** synthesized by mutant I104F/N196W.

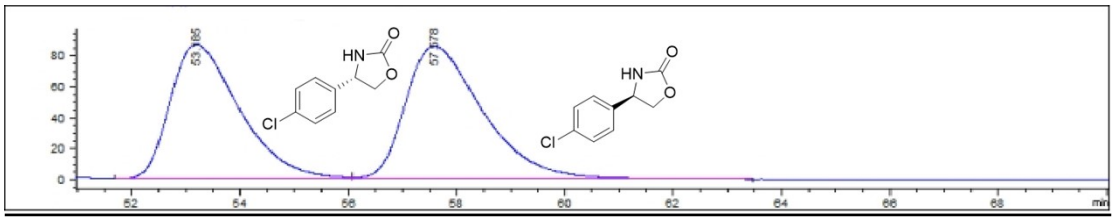

ID#	Ret.Time	Area	Height	Area %
1	53.185	7820.1	87	47.588
2	57.578	8613	86	52.412

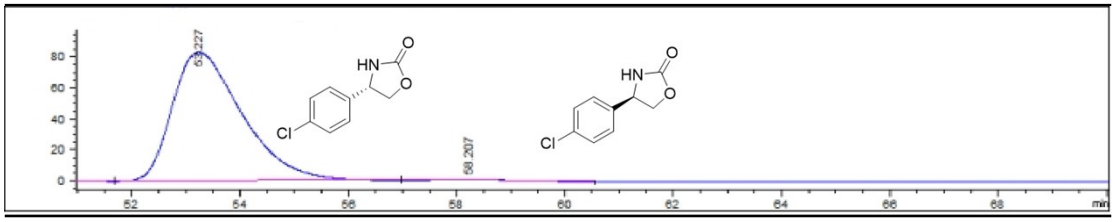

ID#	Ret.Time	Area	Height	Area %
1	53.227	7531.5	83.5	98.822
2	58.207	89.8	1.1	1.178

The *ee* was determined by chiral HPLC (Chiralpak OD-H, *n*-hexane/*i*-PrOH = 90/10, flow rate 0.6 mL/min, λ = 220 nm, t(*S*)-**2i**= 53.2 min, t(*R*)-**2i**= 58.2 min).

Fig. S10 HPLC chromatograms of *rac*-**2i** synthesized by *Ic*HheG, (*S*)-**2i** synthesized by mutant I104F/N196W.

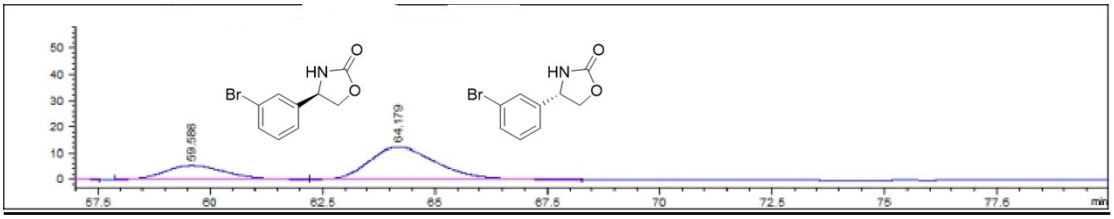

ID#	Ret.Time	Area	Height	Area %
1	59.586	510.5	5.4	28.061
2	64.179	1308.9	12.5	71.939

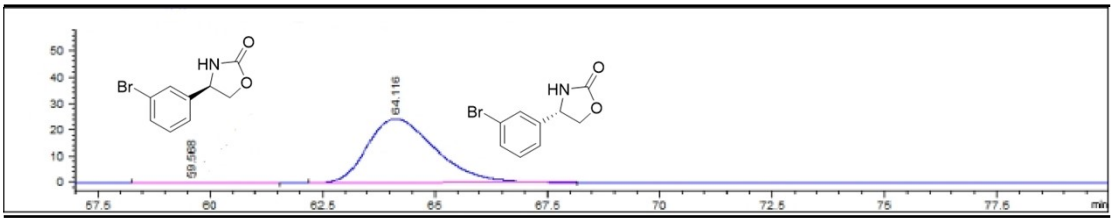

ID#	Ret.Time	Area	Height	Area %
1	59.568	29.5	3E-1	1.112
2	64.116	2619.7	24.6	98.888

The *ee* was determined by chiral HPLC (Chiralpak OD-H, *n*-hexane/*i*-PrOH = 90/10, flow rate 0.6 mL/min, λ = 220 nm, t(*S*)-**2j**= 64.1min, t(*R*)-**2j**= 59.6 min).

Fig. S11 HPLC chromatograms of *rac*-**2j** synthesized by *Ic*HheG, (*S*)-**2j** synthesized by mutant I104F/N196W.

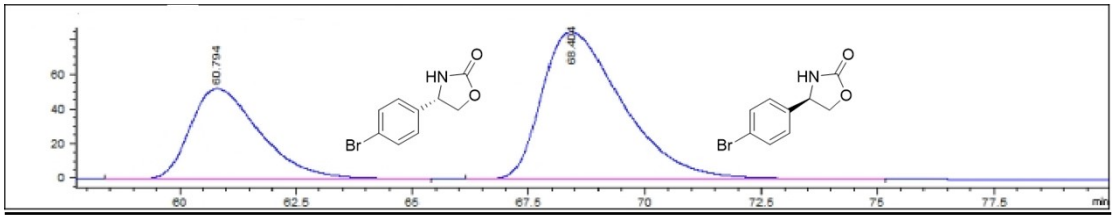

ID#	Ret.Time	Area	Height	Area %
1	60.794	5470.3	52.2	34.679
2	68.404	10303.9	85.1	65.321

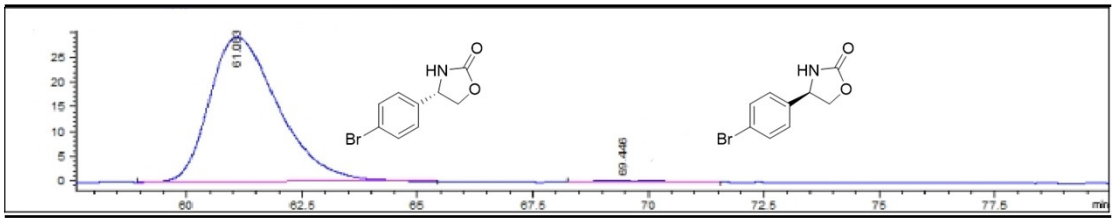

ID#	Ret.Time	Area	Height	Area %
1	61.083	3060.2	29.3	98.995
2	69.446	31.1	3.7E-1	1.005

The *ee* was determined by chiral HPLC (Chiralpak OD-H, *n*-hexane/*i*-PrOH = 90/10, flow rate 0.6 mL/min, λ = 220 nm, t(*S*)-**2k** = 61.1min, t(*R*)-**2k** = 69.4 min).

Fig. S12 HPLC chromatograms of *rac*-**2k** synthesized by *Ic*HheG, (*S*)-**2k** synthesized by mutant I104F/N196W.

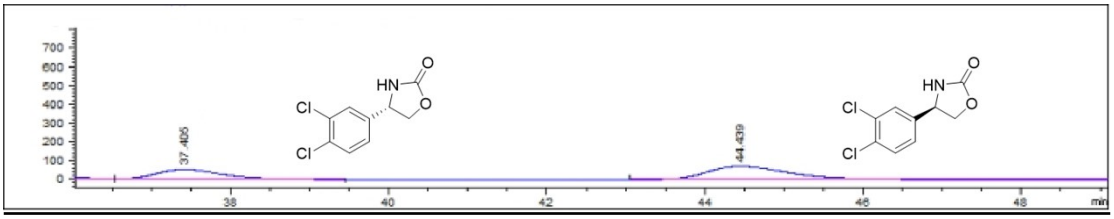

ID#	Ret.Time	Area	Height	Area %
1	37.405	3150.7	53.4	37.658
2	44.439	5215.9	71.8	62.342

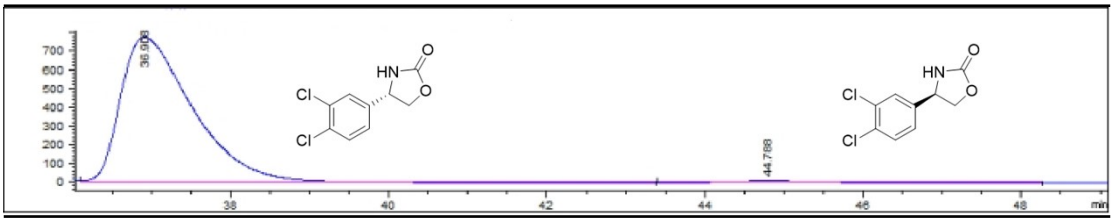

ID#	Ret.Time	Area	Height	Area %
1	36.908	49696.2	778.5	98.625
2	44.788	692.8	9.5	1.375

The *ee* was determined by chiral HPLC (Chiralpak OD-H, *n*-hexane/*i*-PrOH = 80/20, flow rate 0.4 mL/min, λ = 220 nm, t(*S*)-**2l** = 36.9min, t(*R*)-**2l** = 44.8 min).

Fig. S13 HPLC chromatograms of *rac*-**2l** synthesized by *Ic*HheG, (*S*)-**2l** synthesized by mutant I104F/N196W.

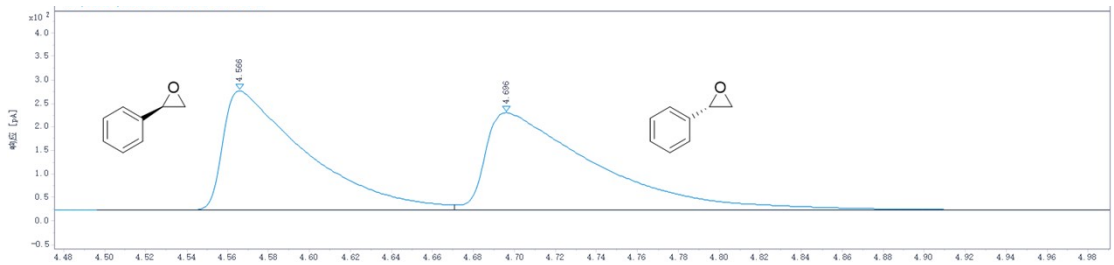

ID #	RT (min)	Area %	Area (pA·s)	Height (pA)
1	4.566	47.877	713.357	253.697
2	4.696	52.123	776.625	207.428

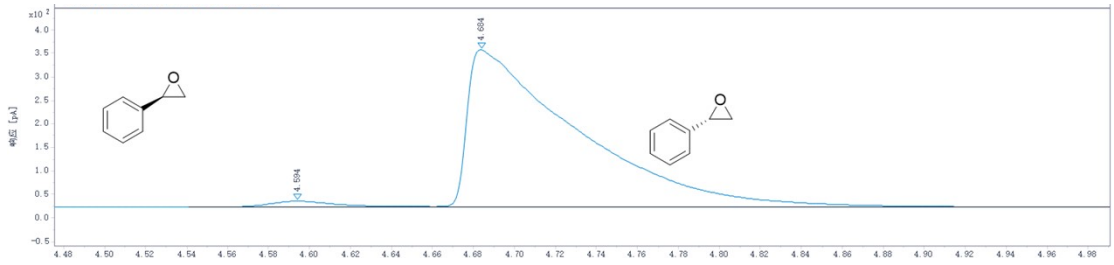

ID #	RT (min)	Area %	Area (pA·s)	Height (pA)
1	4.594	2.387	30.730	12.527
2	4.684	97.613	1256.631	334.609

The detection method is as follows: start at 100 ℃, increase at 5 ℃/min to 180 ℃, and hold at 10 ℃/min increase to 220 ℃ for 8 minutes.

Fig. S14 Chiral GC chromatograms of *rac*-**1a**; Chiral GC chromatogram analysis of biotransformation of *rac*-**1a** by mutant I104F/N196W.

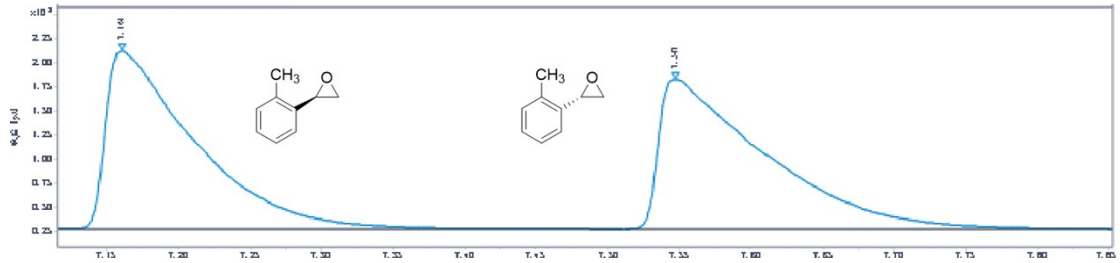

ID #	RT (min)	Area %	Area (pA·s)	Height (pA)
1	7.161	49.967	799.388	185.014
2	7.547	50.033	800.440	155.289

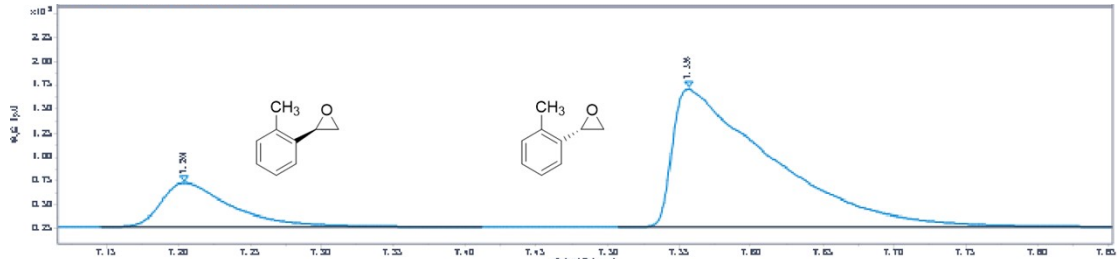

ID #	RT (min)	Area %	Area (pA·s)	Height (pA)
1	7.204	18.762	161.283	46.295
2	7.556	81.238	698.364	144.572

The detection method is as follows: start at 100 ℃, increase at 3 ℃/min to 180 ℃, and hold at 10 ℃/min increase to 220 ℃ for 8 minutes.

Fig. S15 Chiral GC chromatograms of *rac*-**1b**; Chiral GC chromatogram analysis of biotransformation of *rac*-**1b** by mutant I104F/N196W.

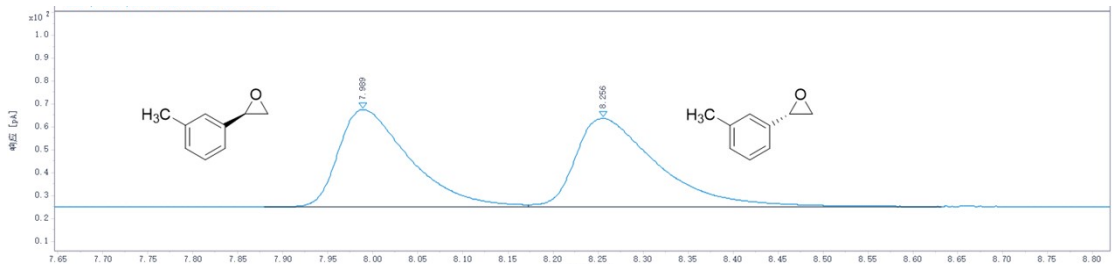

ID #	RT (min)	Area %	Area (pA·s)	Height (pA)
1	7.989	48.897	232.551	42.449
2	8.256	51.103	243.046	38.559

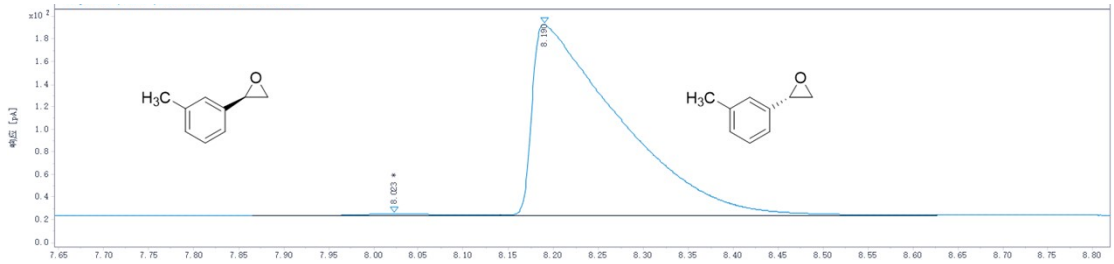

ID #	RT (min)	Area %	Area (pA·s)	Height (pA)
1	8.023	0.726	8.265	1.502
2	8.190	99.274	1130.286	169.295

The detection method is as follows: start at 100 ℃, increase at 1 ℃/min to 160 ℃, and hold at 20 ℃/min increase to 220 ℃ for 8 minutes.

Fig. S16 Chiral GC chromatograms of *rac*-**1c**; Chiral GC chromatogram analysis of biotransformation of *rac*-**1c** by mutant I104F/N196W.

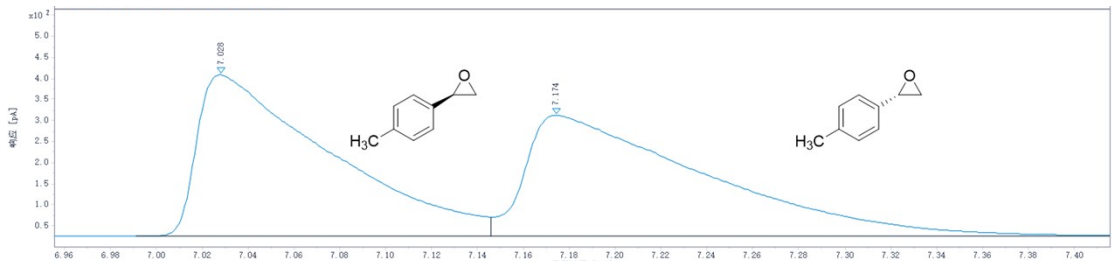

ID #	RT (min)	Area %	Area (pA·s)	Height (pA)
1	7.028	49.569	1534.727	383.411
2	7.174	50.431	1561.407	286.935

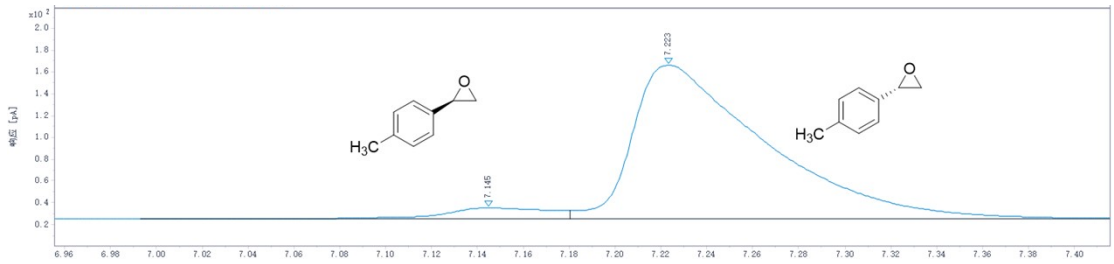

ID #	RT (min)	Area %	Area (pA·s)	Height (pA)
1	7.145	5.733	35.165	10.374
2	7.223	94.267	578.176	141.498

The detection method is as follows: start at 100 ℃, increase at 3 ℃/min to 180 ℃, and hold at 10 ℃/min increase to 220 ℃ for 8 minutes.

Fig. S17 Chiral GC chromatograms of *rac*-**1d**; Chiral GC chromatogram analysis of biotransformation of *rac*-**1d** by mutant I104F/N196W.

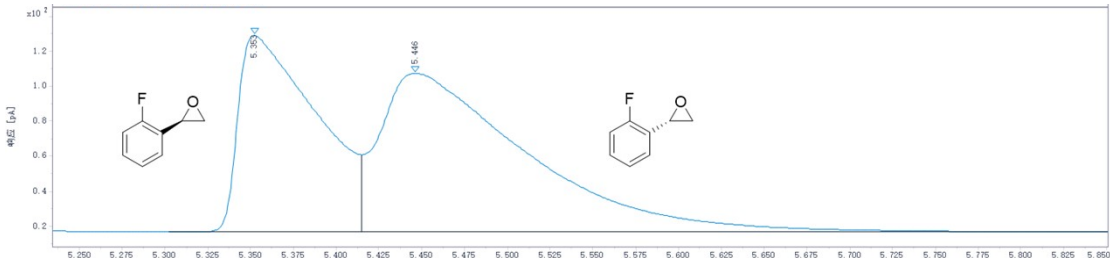

ID #	RT (min)	Area %	Area (pA·s)	Height (pA)
1	5.353	39.522	357.518	112.202
2	5.446	60.478	547.085	90.513

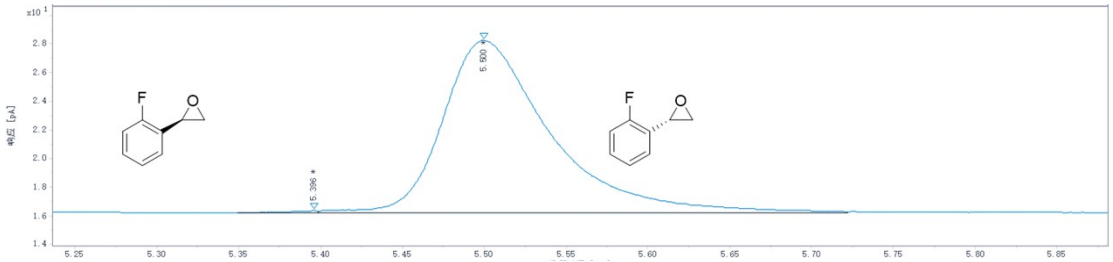

ID #	RT (min)	Area %	Area (pA·s)	Height (pA)
1	5.396	1.708	0.950	0.560
2	5.500	98.292	54.646	12.044

The detection method is as follows: start at 100 ℃, increase at 0.5 ℃/min to 115 ℃, and hold at 10 ℃/min increase to 220 ℃ for 8 minutes.

Fig. S18 Chiral GC chromatograms of *rac*-**1e**; Chiral GC chromatogram analysis of biotransformation of *rac*-**1e** by mutant I104F/N196W.

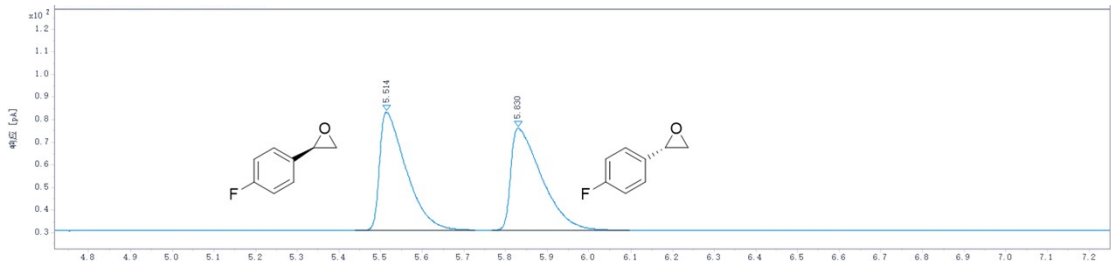

ID #	RT (min)	Area %	Area (pA·s)	Height (pA)
1	5.514	50.059	233.076	52.329
2	5.830	49.941	232.529	45.216

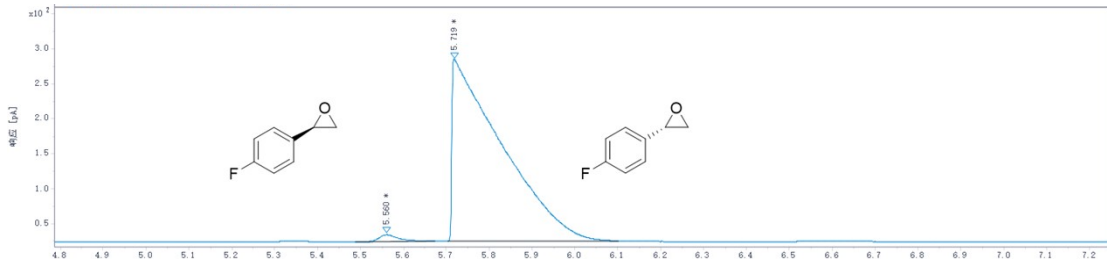

ID #	RT (min)	Area %	Area (pA·s)	Height (pA)
1	5.560	1.465	31.284	9.879
2	5.719	98.535	2103.844	259.444

The detection method is as follows: start at 100 ℃, increase at 5 ℃/min to 180 ℃, and hold at 10 ℃/min increase to 220 ℃ for 8 minutes.

Fig. S19 Chiral GC chromatograms of *rac*-**1f**; Chiral GC chromatogram analysis of biotransformation of *rac*-**1f** by mutant I104F/N196W.

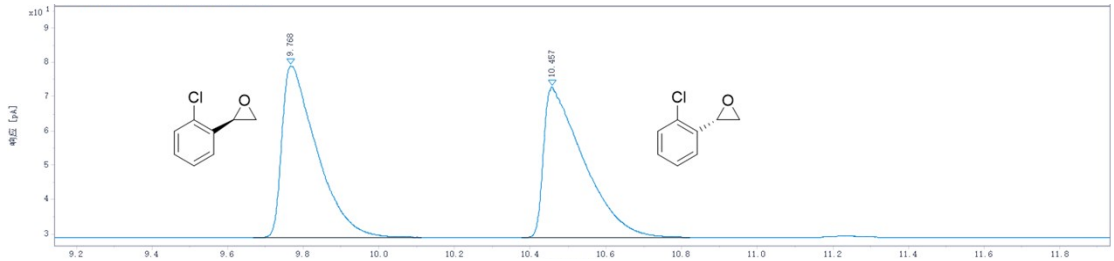

ID #	RT (min)	Area %	Area (pA·s)	Height (pA)
1	9.768	50.066	322.484	50.067
2	10.457	49.934	321.634	43.985

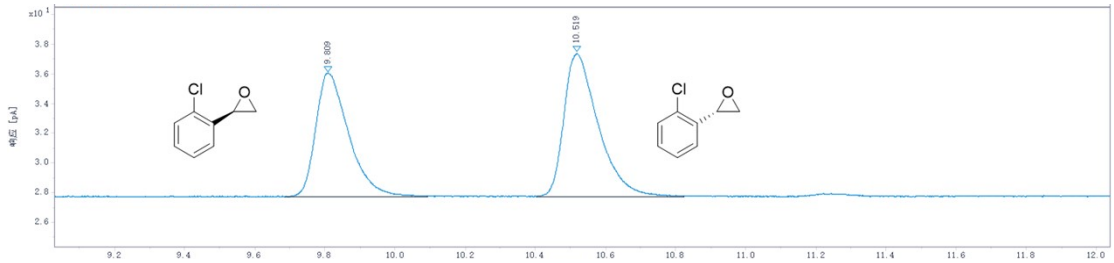

ID #	RT (min)	Area %	Area (pA·s)	Height (pA)
1	9.809	45.413	54.530	8.337
2	10.519	54.587	65.546	9.648

The detection method is as follows: start at 100 ℃, increase at 1 ℃/min to 160 ℃, and hold at 20 ℃/min increase to 220 ℃ for 8 minutes.

Fig. S20 Chiral GC chromatograms of *rac*-**1g**; Chiral GC chromatogram analysis of biotransformation of *rac*-**1g** by mutant I104F/N196W.

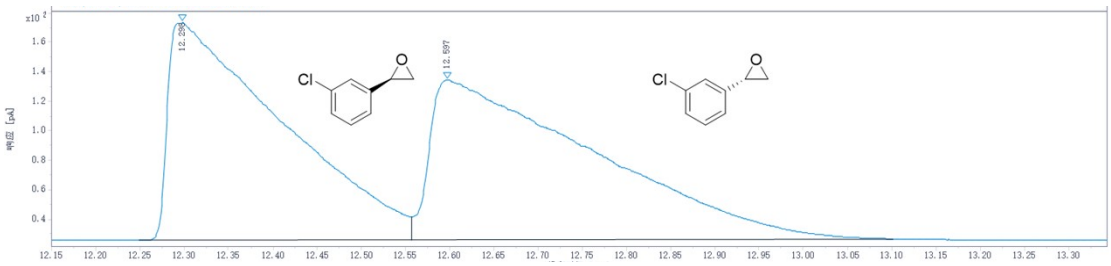

ID #	RT (min)	Area %	Area (pA·s)	Height (pA)
1	12.298	48.601	1323.352	147.667
2	12.597	51.399	1399.521	108.570

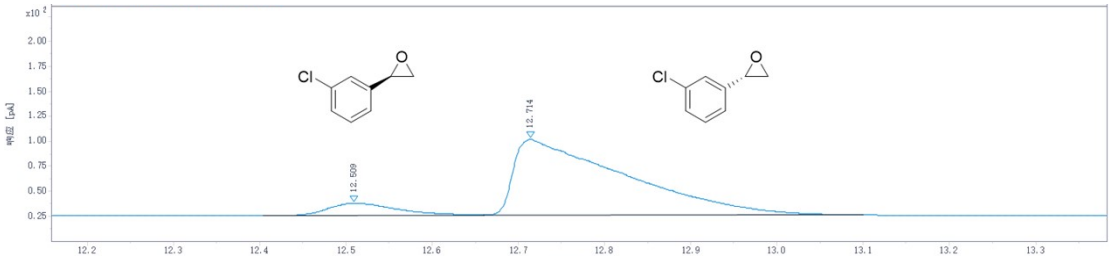

ID #	RT (min)	Area %	Area (pA·s)	Height (pA)
1	12.509	9.238	69.578	12.365
2	12.714	90.762	683.581	75.855

The detection method is as follows: start at 100 ℃, increase at 5 ℃/min to 180 ℃, and hold at 10 ℃/min increase to 220 ℃ for 8 minutes.

Fig. S21 Chiral GC chromatograms of *rac*-**1h**; Chiral GC chromatogram analysis of biotransformation of *rac*-**1h** by mutant I104F/N196W.

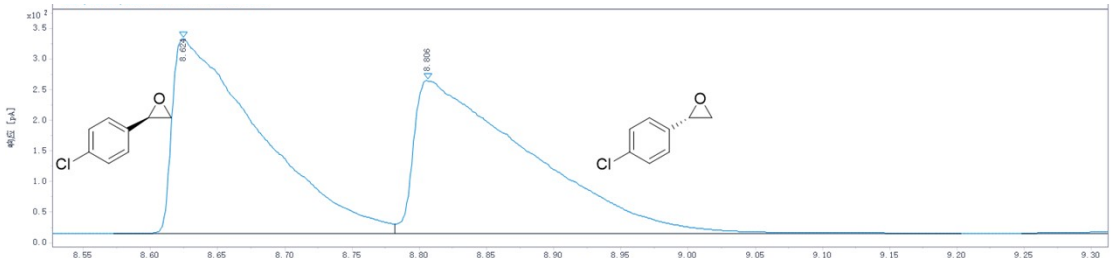

ID #	RT (min)	Area %	Area (pA·s)	Height (pA)
1	8.624	49.342	1439.877	318.291
2	8.806	50.658	1478.257	249.414

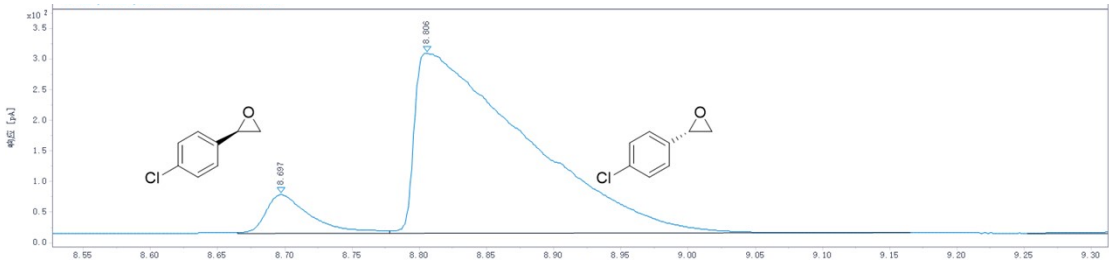

ID #	RT (min)	Area %	Area (pA·s)	Height (pA)
1	8.697	7.865	145.538	62.876
2	8.806	92.135	1704.952	293.672

The detection method is as follows: start at 100℃, increase at 2℃/min to 180 ℃, and hold at 20 ℃/min increase to 220 ℃ for 8 minutes.

Fig. S22 Chiral GC chromatograms of *rac*-**1i**; Chiral GC chromatogram analysis of biotransformation of *rac*-**1i** by mutant I104F/N196W.

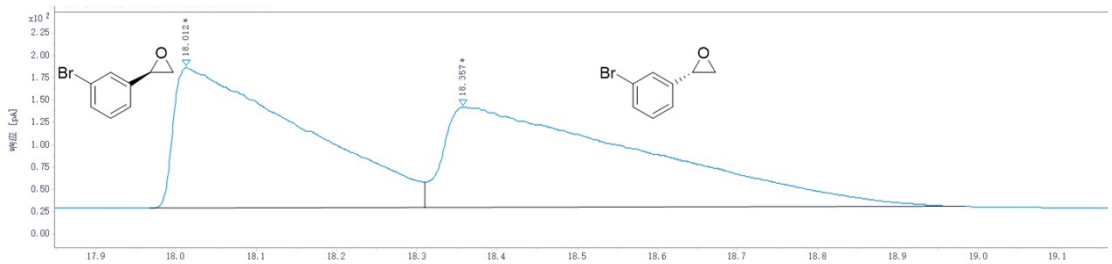

ID #	RT (min)	Area %	Area (pA·s)	Height (pA)
1	18.012	47.343	1773.425	157.664
2	18.357	52.657	1972.465	112.689

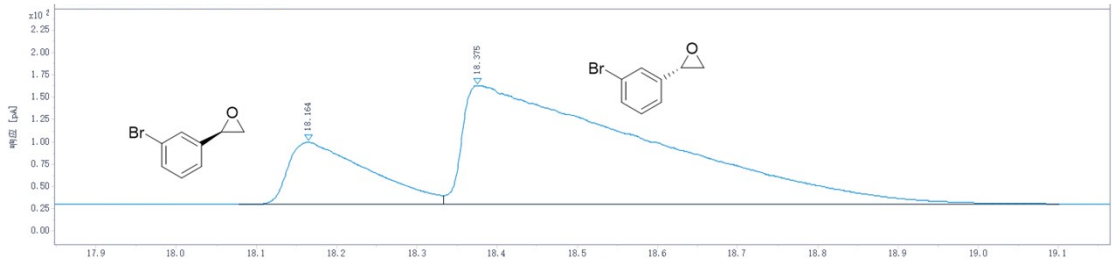

ID #	RT (min)	Area %	Area (pA·s)	Height (pA)
1	18.164	18.576	487.419	69.778
2	18.375	81.424	2136.539	133.119

The detection method is as follows: start at 100 ℃, increase at 1 ℃/min to 160 ℃, and hold at 20 ℃/min increase to 220 ℃ for 8 minutes.

Fig. S23 Chiral GC chromatograms of *rac*-**1j**; Chiral GC chromatogram analysis of biotransformation of *rac*-**1j** by mutant I104F/N196W.

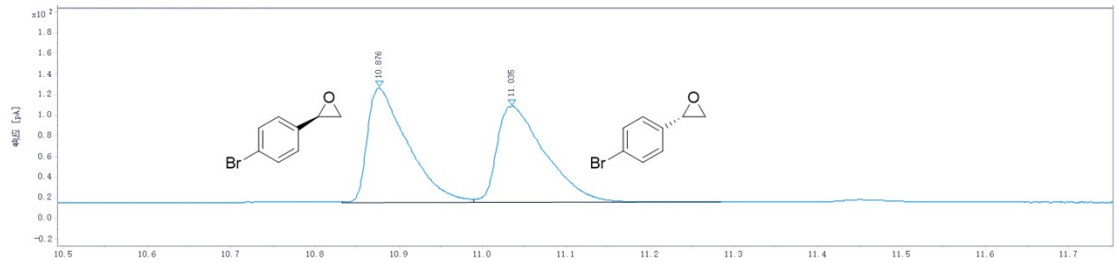

ID #	RT (min)	Area %	Area (pA·s)	Height (pA)
1	10.876	49.870	368.406	110.566
2	11.035	50.130	370.406	92.998

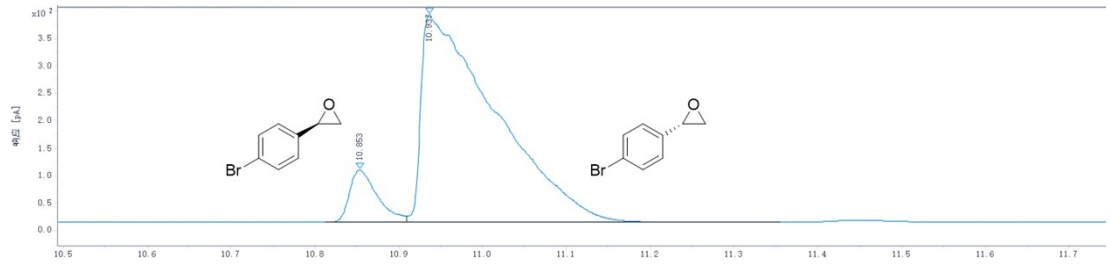

ID #	RT (min)	Area %	Area (pA·s)	Height (pA)
1	10.853	8.619	219.867	95.091
2	10.937	91.381	2330.995	377.454

The detection method is as follows: start at 100 ℃, increase at 5 ℃/min to 180 ℃, and hold at 10 ℃/min increase to 220 ℃ for 8 minutes.

Fig. S24 Chiral GC chromatograms of *rac*-**1k**; Chiral GC chromatogram analysis of biotransformation of *rac*-**1k** by mutant I104F/N196W.

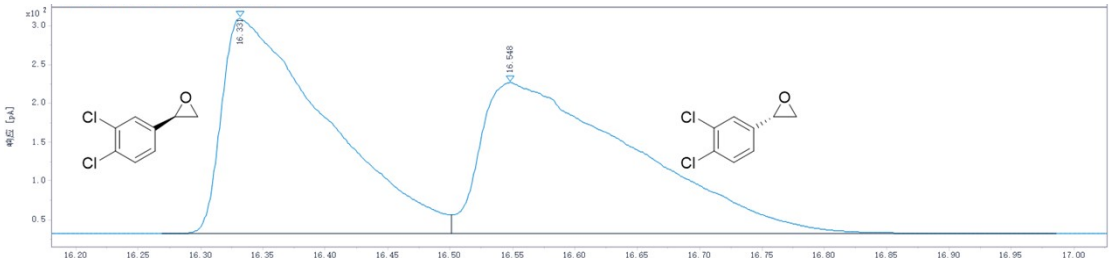

ID #	RT (min)	Area %	Area (pA·s)	Height (pA)
1	16.331	49.073	1620.512	277.498
2	16.548	50.927	1681.705	194.873

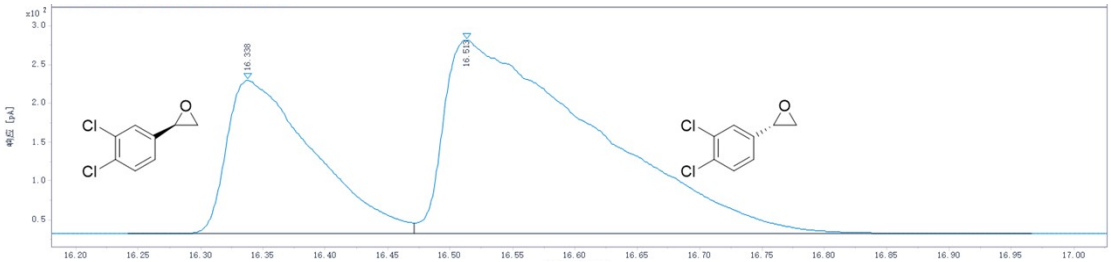

ID #	RT (min)	Area %	Area (pA·s)	Height (pA)
1	16.338	31.297	958.400	197.501
2	16.513	68.703	2103.826	249.580

The detection method is as follows: start at 100 ℃, increase at 3 ℃/min to 180 ℃, and hold at 10 ℃/min increase to 220 ℃ for 8 minutes.

Fig. S25 Chiral GC chromatograms of *rac*-**1l**; Chiral GC chromatogram analysis of biotransformation of *rac*-**1l** by mutant I104F/N196W.

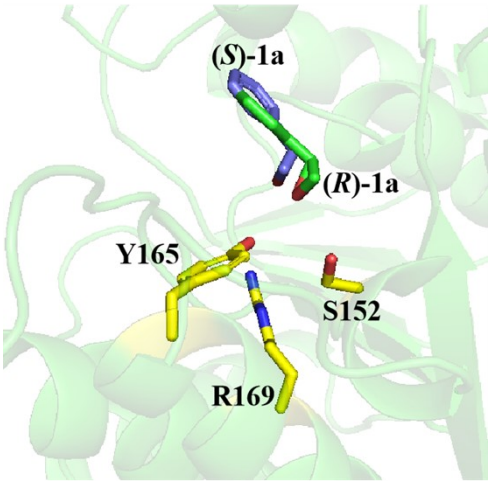

Fig. S26 Docking analysis of *Ic*HheG with **1a**.

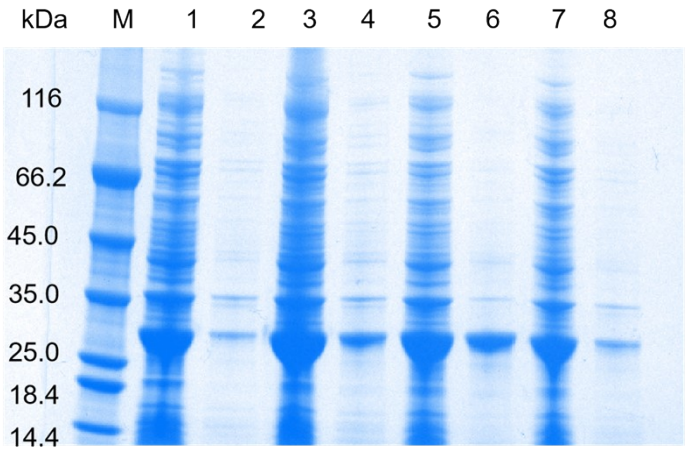

Fig. S27 SDS-PAGE analysis of overexpression of the recombinant *E. coli* (*Ic*HheG) and its mutants. Lane M: protein marker; Lane **1**: the supernatant of *E. coli* (*Ic*HheG); Lane **2**: the deposit of *E. coli* (*Ic*HheG); Lane **3**: the supernatant of *E. coli* (N196W); Lane **4**: the deposit of *E. coli* (N196W); Lane **5**: the supernatant of *E. coli* (L103G); Lane **6**: the deposit of *E. coli* (L103G); Lane **7**: the supernatant of *E. coli* (I104F/N196W); Lane **8**: the deposit of *E. coli* (I104F/N196W).

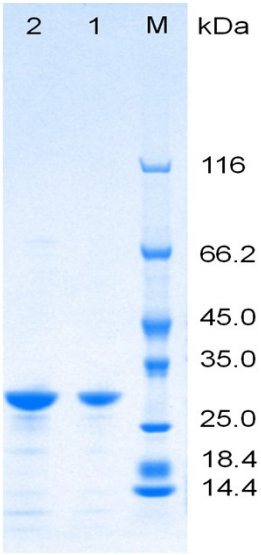

Fig. S28 SDS-PAGE analysis of the purification of *Ic*HheG and mutant I104F/N196W. Lane M: protein marker; Lane 1: purified mutant I104F/N196W; Lane 2: purified *Ic*HheG.

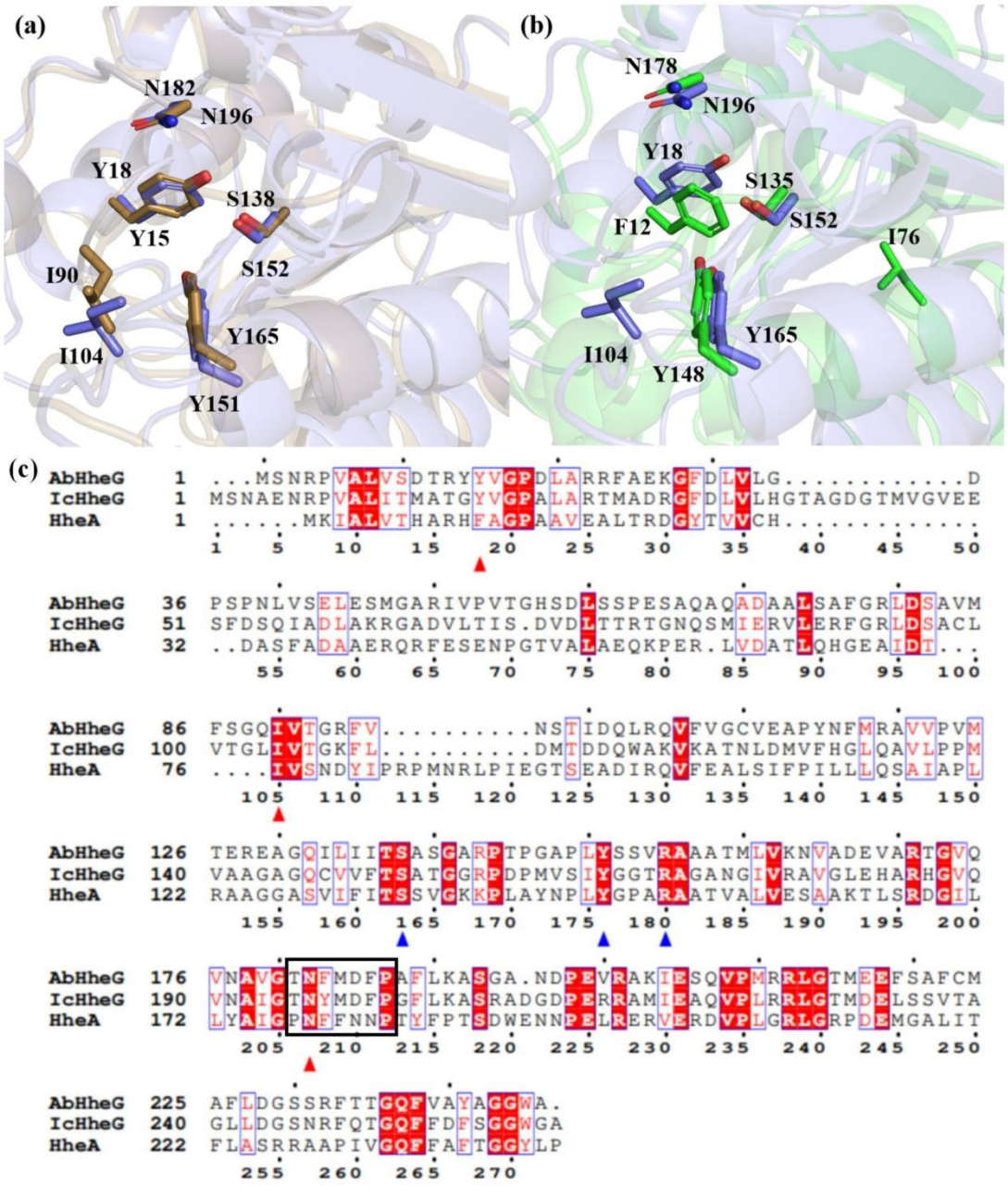

Fig. S29: a: Structural comparison of *Ab*HheG (sand) with *Ic*HheG (deepblue). b: Structural comparison of HheA (green) with *Ic*HheG (deep blue). c: Protein sequence alignment of *Ic*HheG, *Ab*HheG and HheA. Halide binding sites are marked with black box. The catalytic triad are marked by blue triangles. Residues 18 (*Ic*HheG), 15 (*Ab*HheG) and 12 (HheA) are marked by red triangle. Residues 104 (*Ic*HheG), 90 (*Ab*HheG) and 76 (HheA) are marked by red triangle. Residues 196 (*Ic*HheG), 182 (*Ab*HheG) and 178 (HheA) are marked by red triangle.

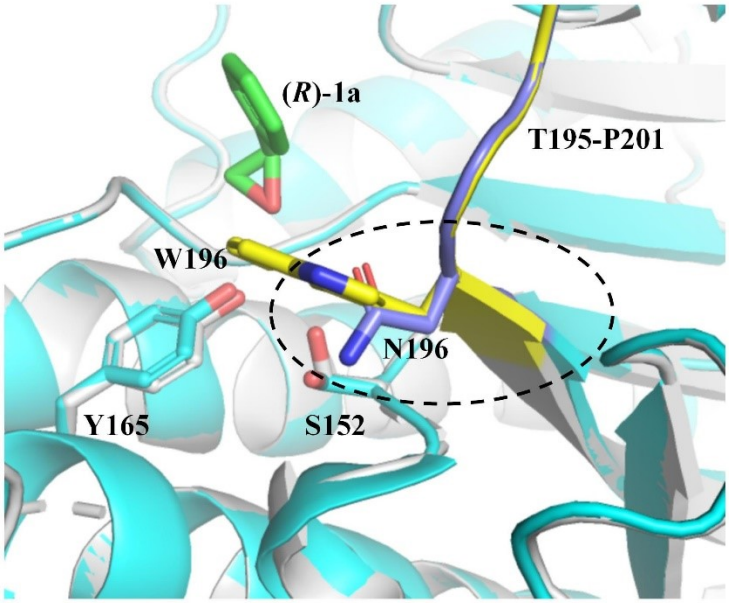

Fig. S30 Structural comparison of WT *Ic*HheG (cyan) with mutant I104F/N196W (grey). Halide binding loop in WT *Ic*HheG (Residues 195-201) is marked with deepblue. Halide binding loop in mutant I104F/N196W (Residues 195-201) is marked with yellow.

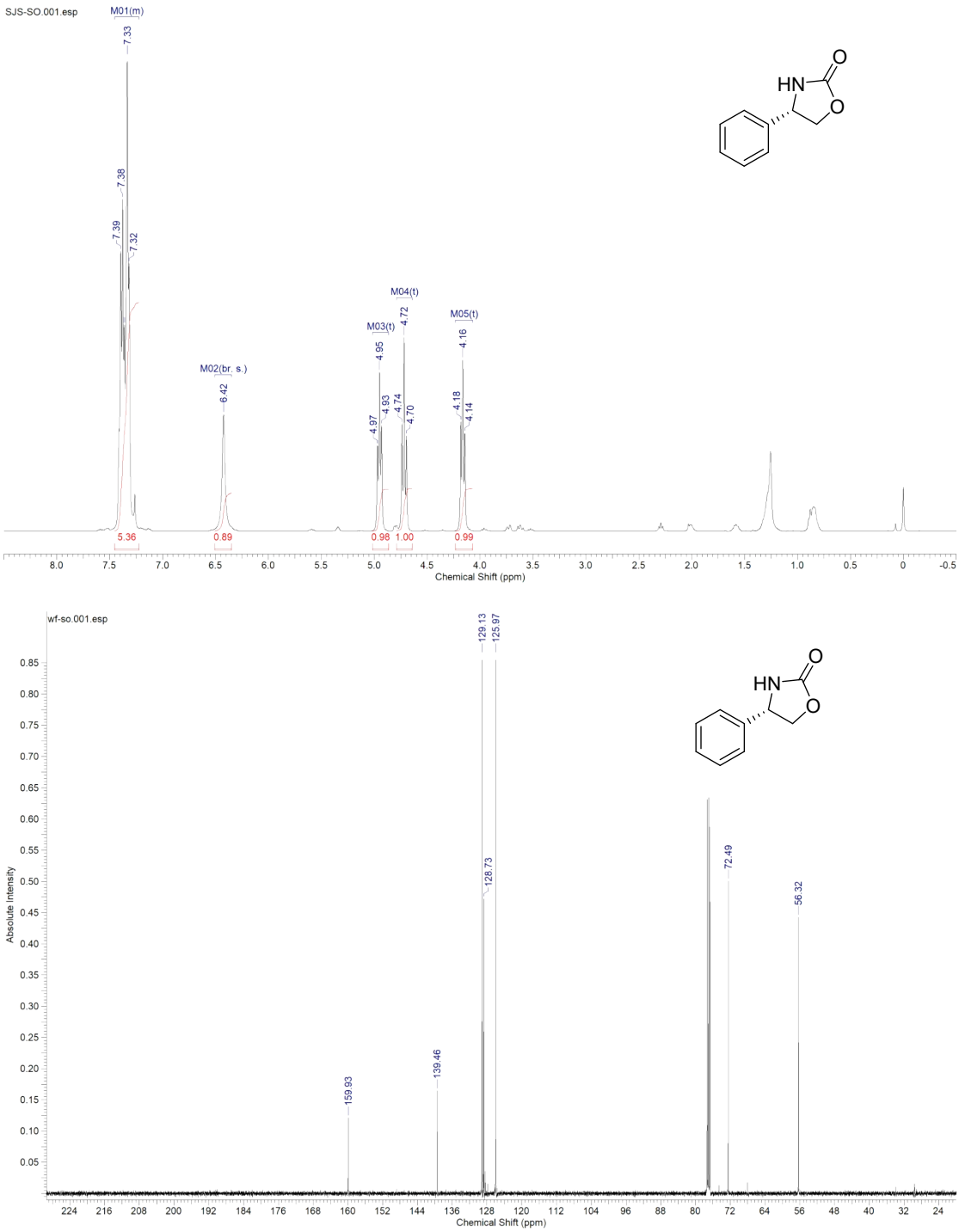

Fig. S31 NMR spectra copies of (*S*)-4-phenyloxazolidin-2-one (**2a**).

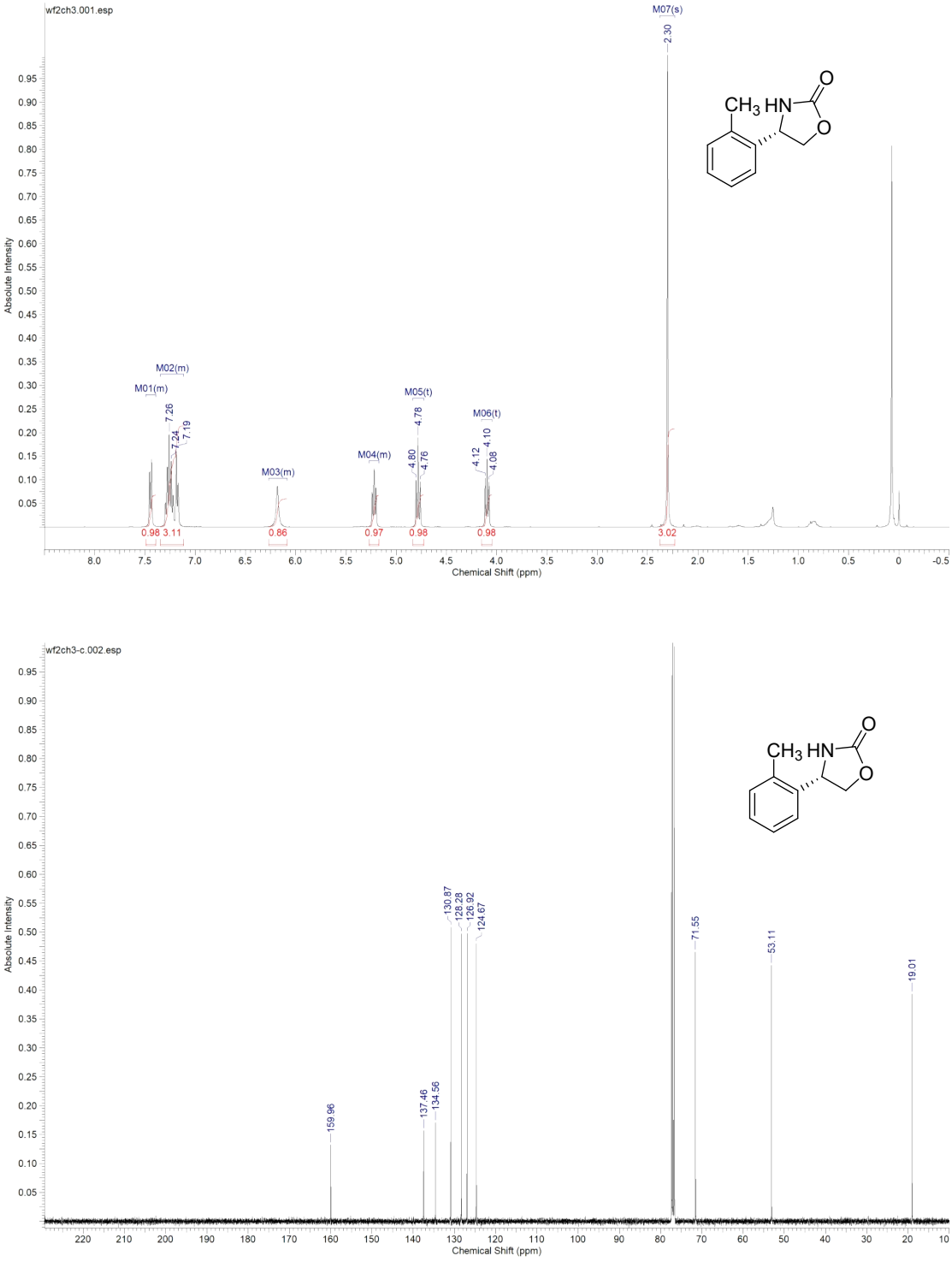

Fig. S32 NMR spectra copies of (*S*)-4-(*o*-tolyl)oxazolidin-2-one (**2b**).

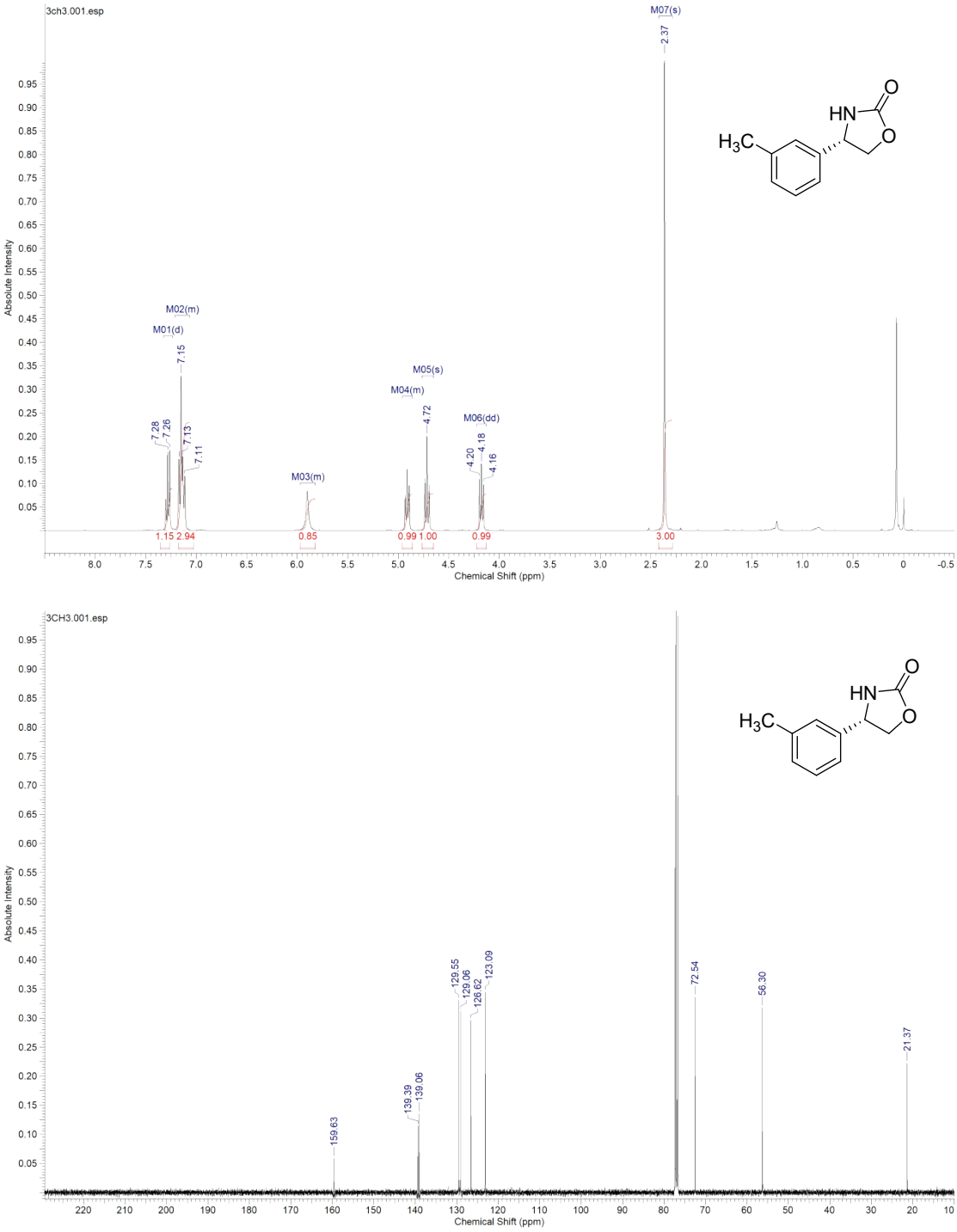

Fig. S33 NMR spectra copies of (*S*)-4-(*p*-tolyl)oxazolidin-2-one (**2c**).

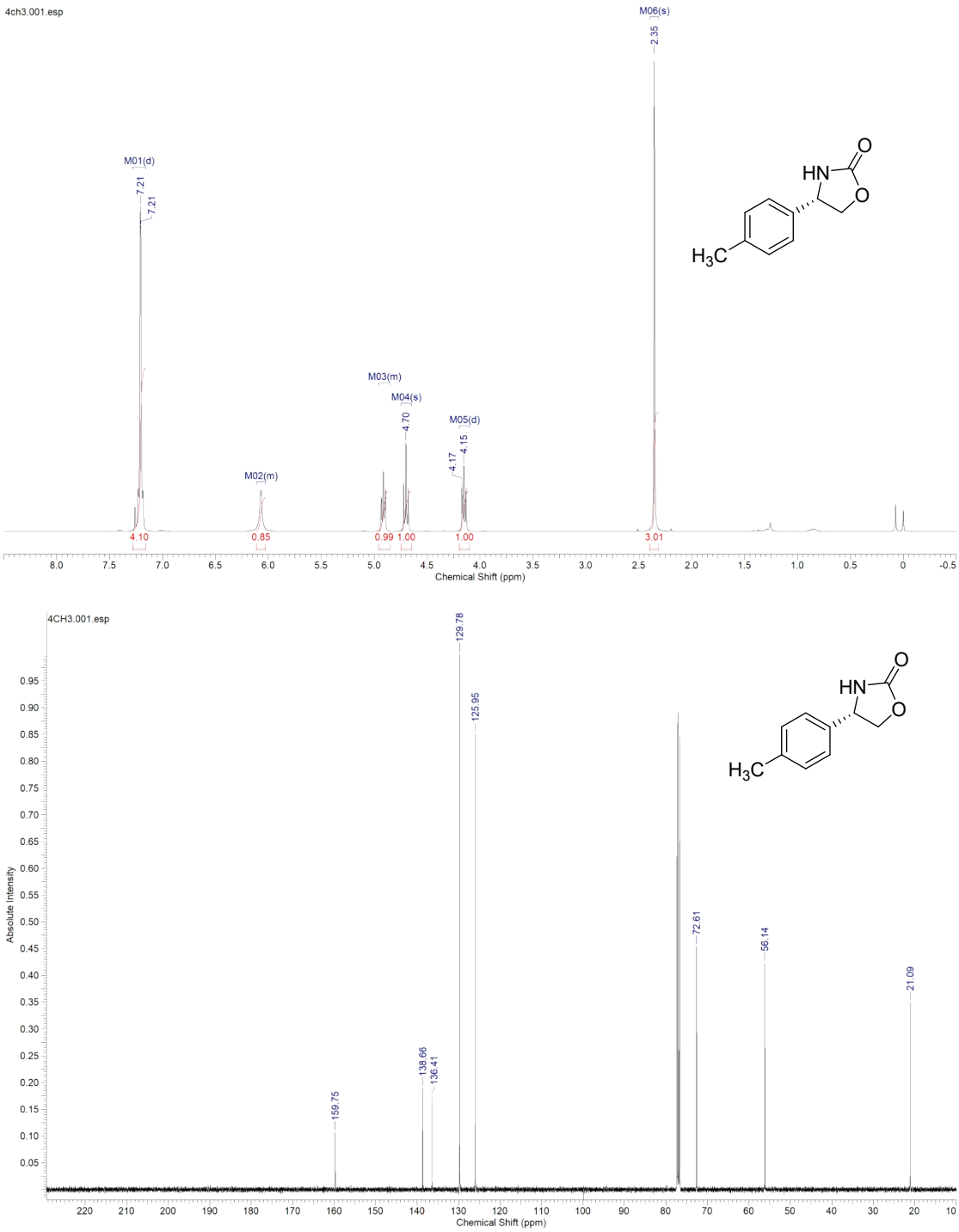

Fig. S34 NMR spectra copies of (*S*)-4-(*p*-tolyl)oxazolidin-2-one (**2d**).

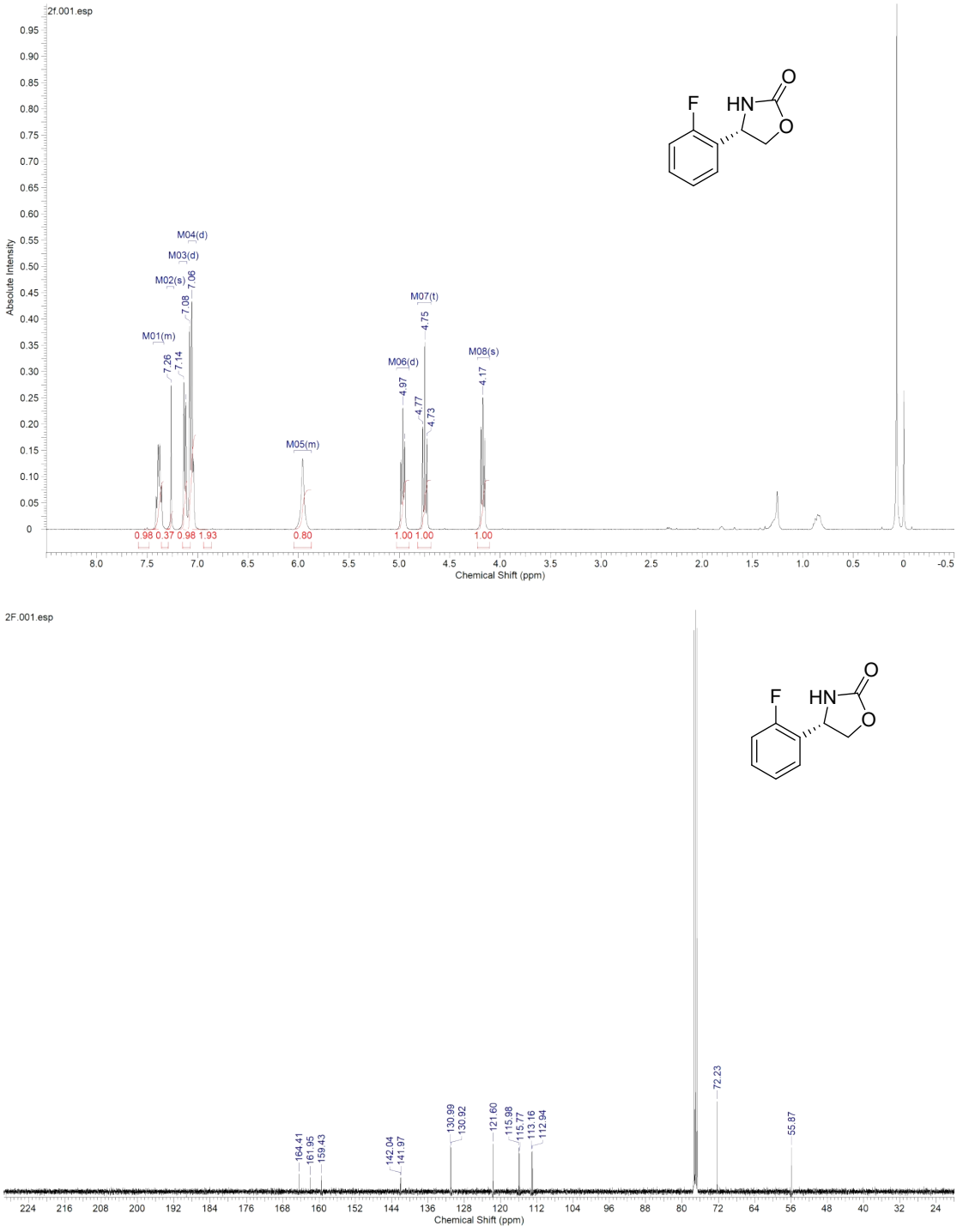

Fig. S35 NMR spectra copies of (*S*)-4-(2-fluorophenyl)oxazolidin-2-one (**2e**).

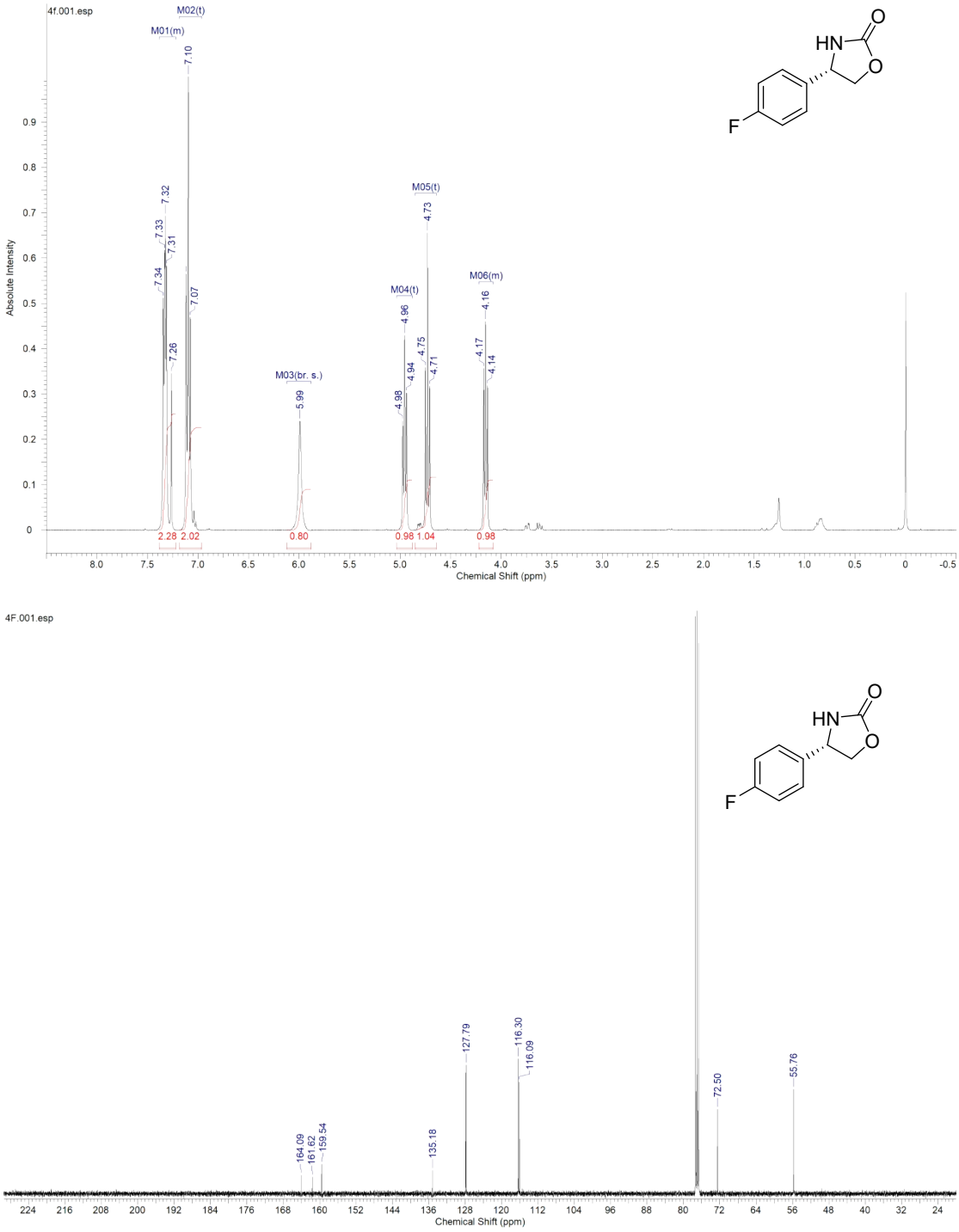

Fig. S36 NMR spectra copies of (*S*)-4-(4-fluorophenyl)oxazolidin-2-one (**2f**).

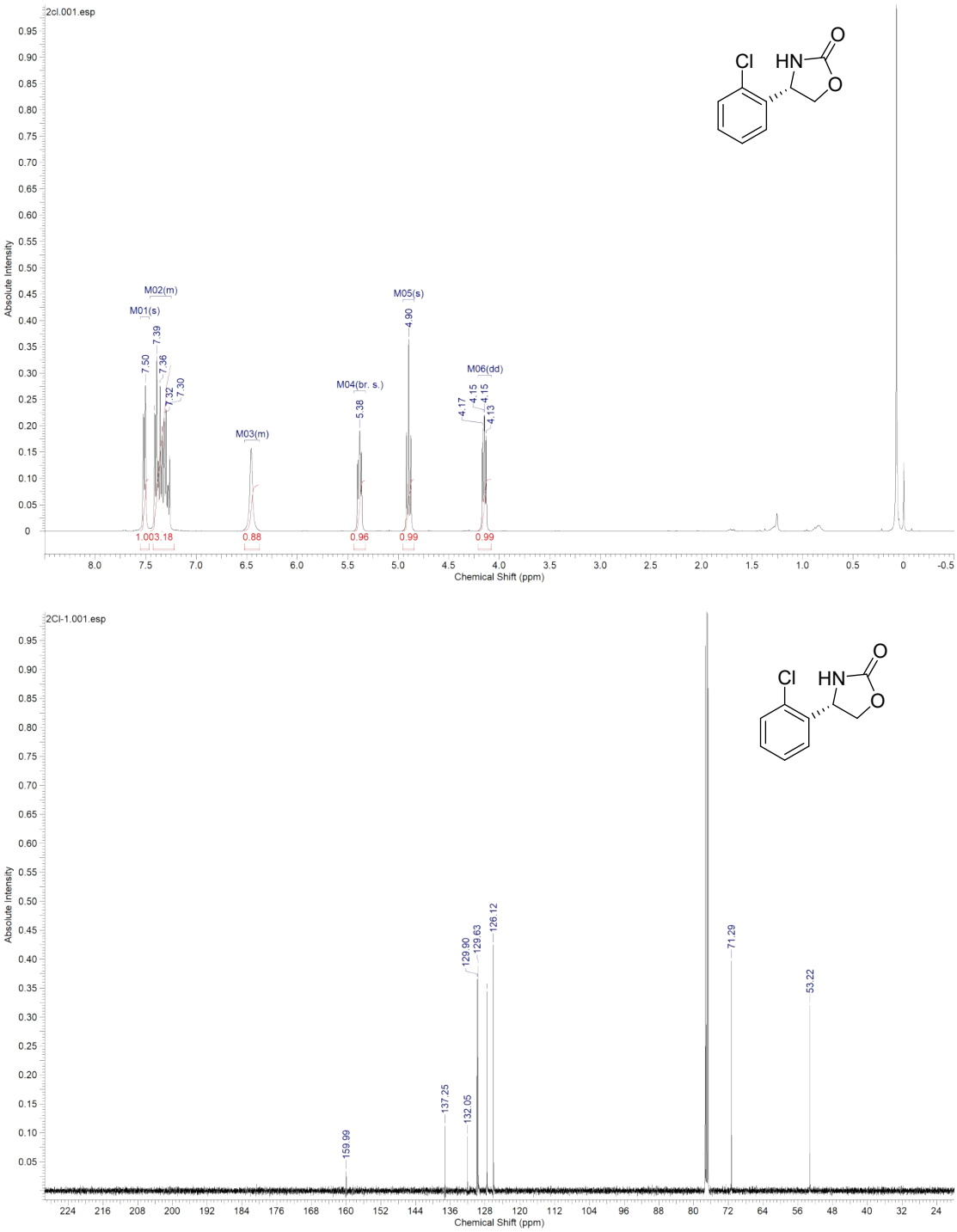

Fig. S37 NMR spectra copies of (*S*)-4-(2-chlorophenyl)oxazolidin-2-one (**2g**).

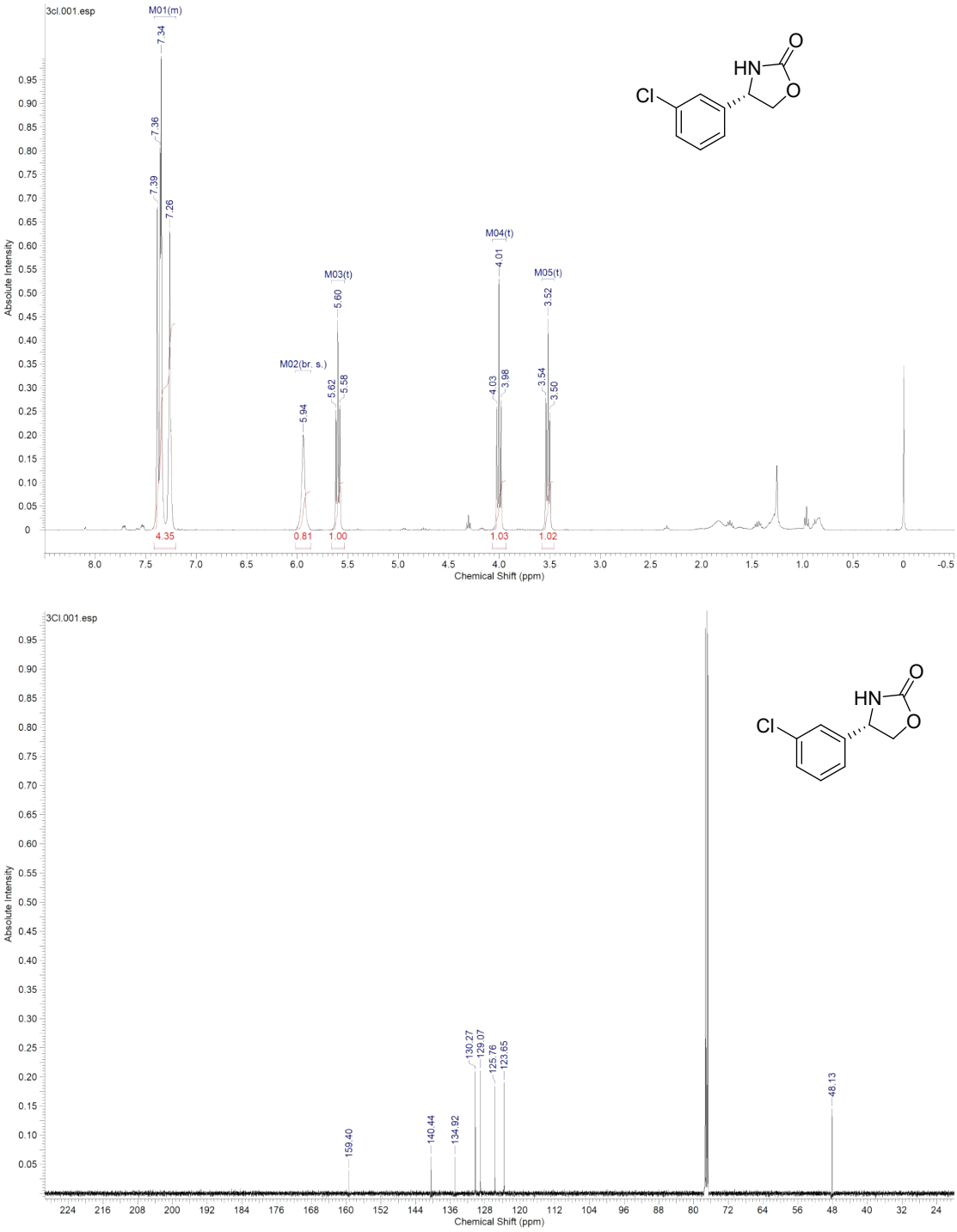

Fig. S38 NMR spectra copies of (*S*)-4-(3-chlorophenyl)oxazolidin-2-one (**2h**).

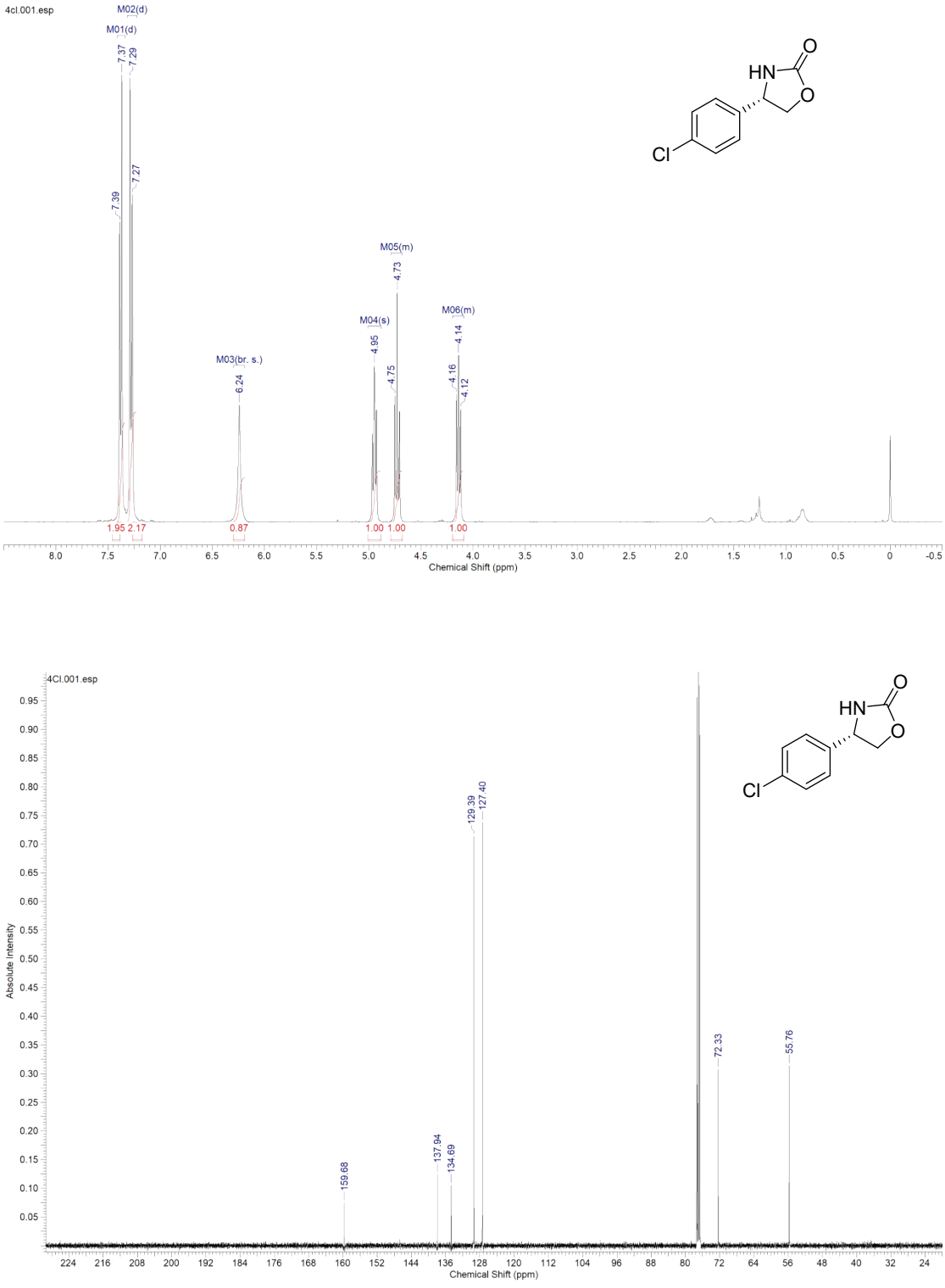

Fig. S39 NMR spectra copies of (*S*)-4-(4-chlorophenyl)oxazolidin-2-one (**2i**).

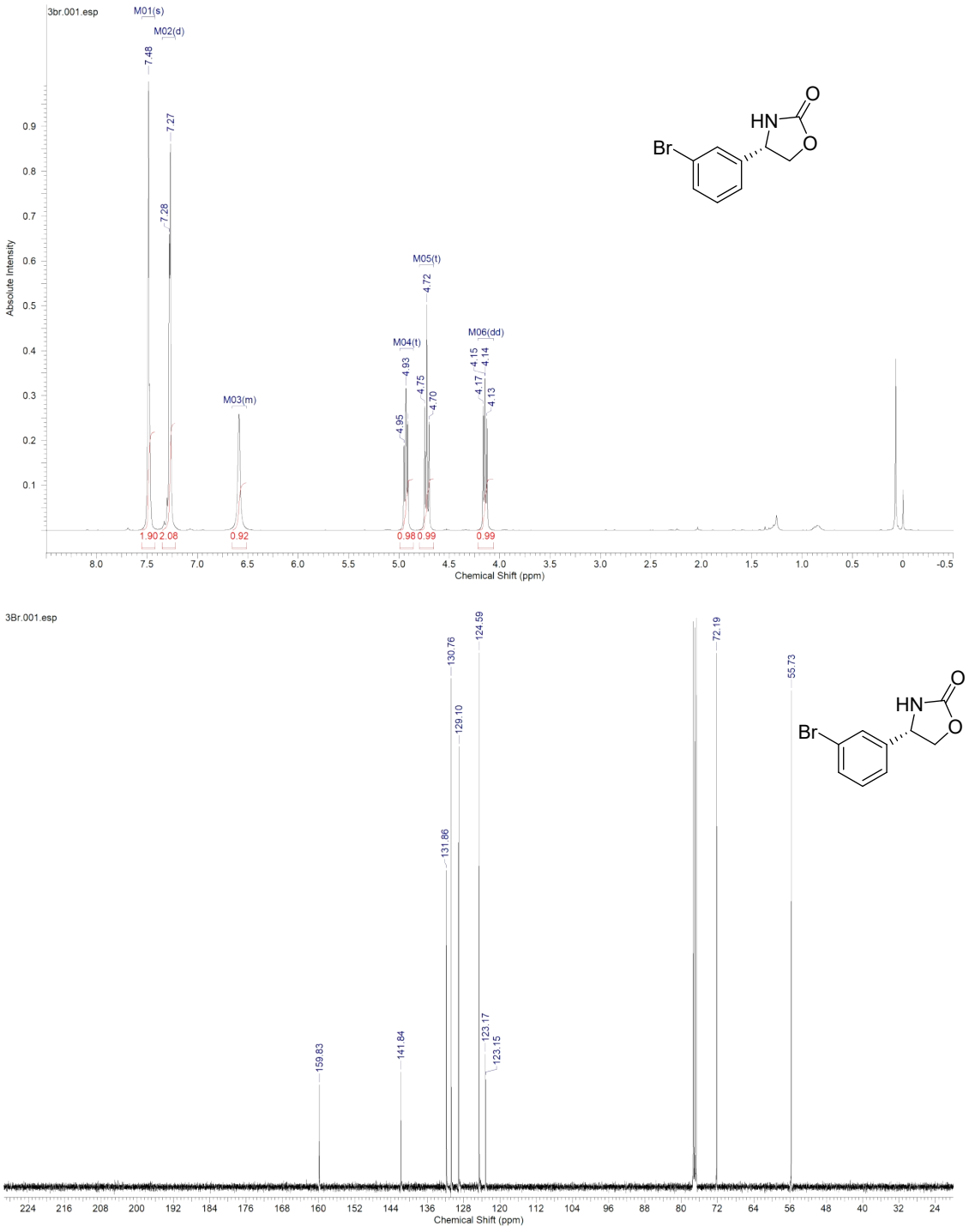

Fig. S40 NMR spectra copies of (*S*)-4-(3-bromophenyl)oxazolidin-2-one (**2j**).

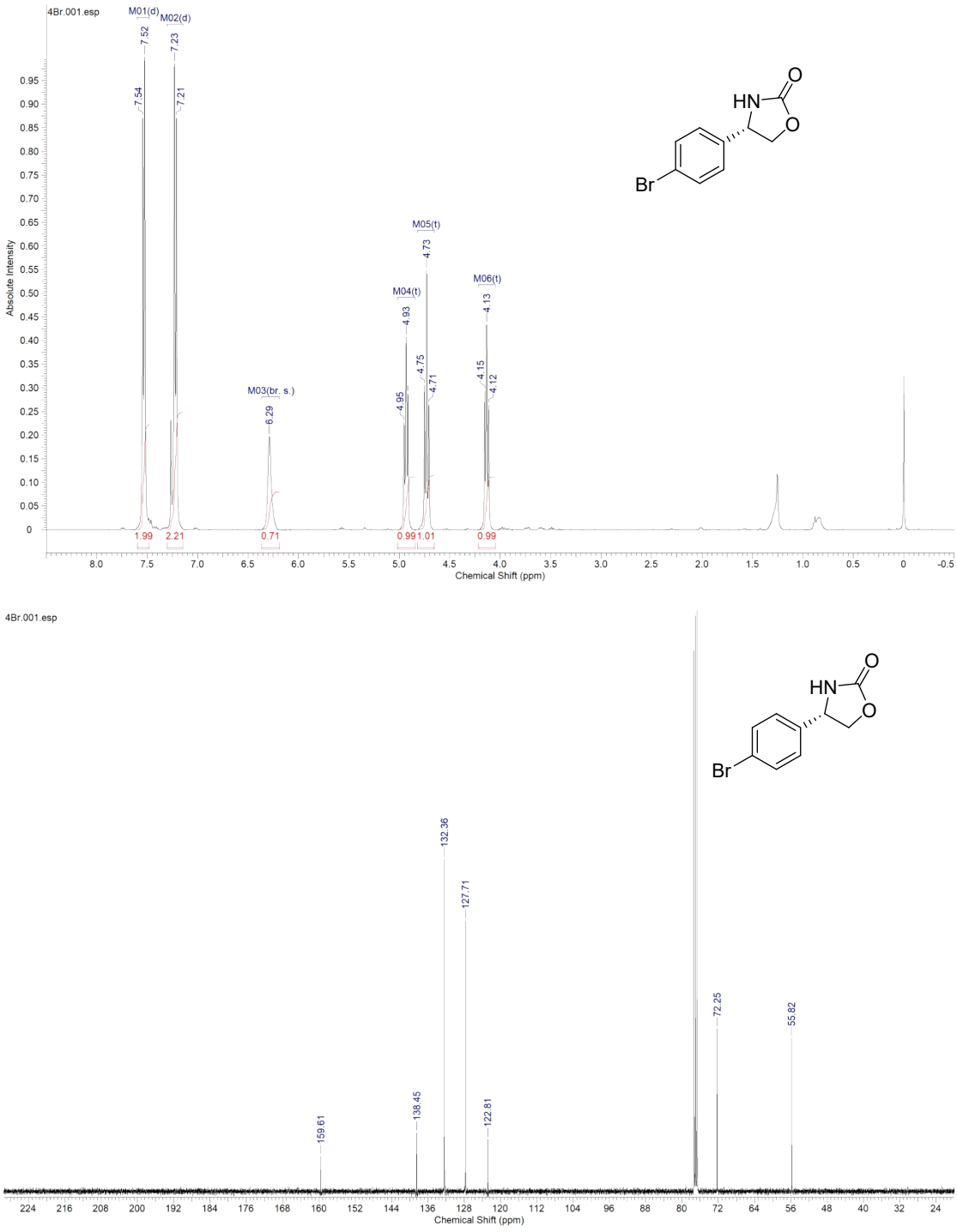

Fig. S41 NMR spectra copies of (*S*)-4-(4-bromophenyl)oxazolidin-2-one (**2k**).

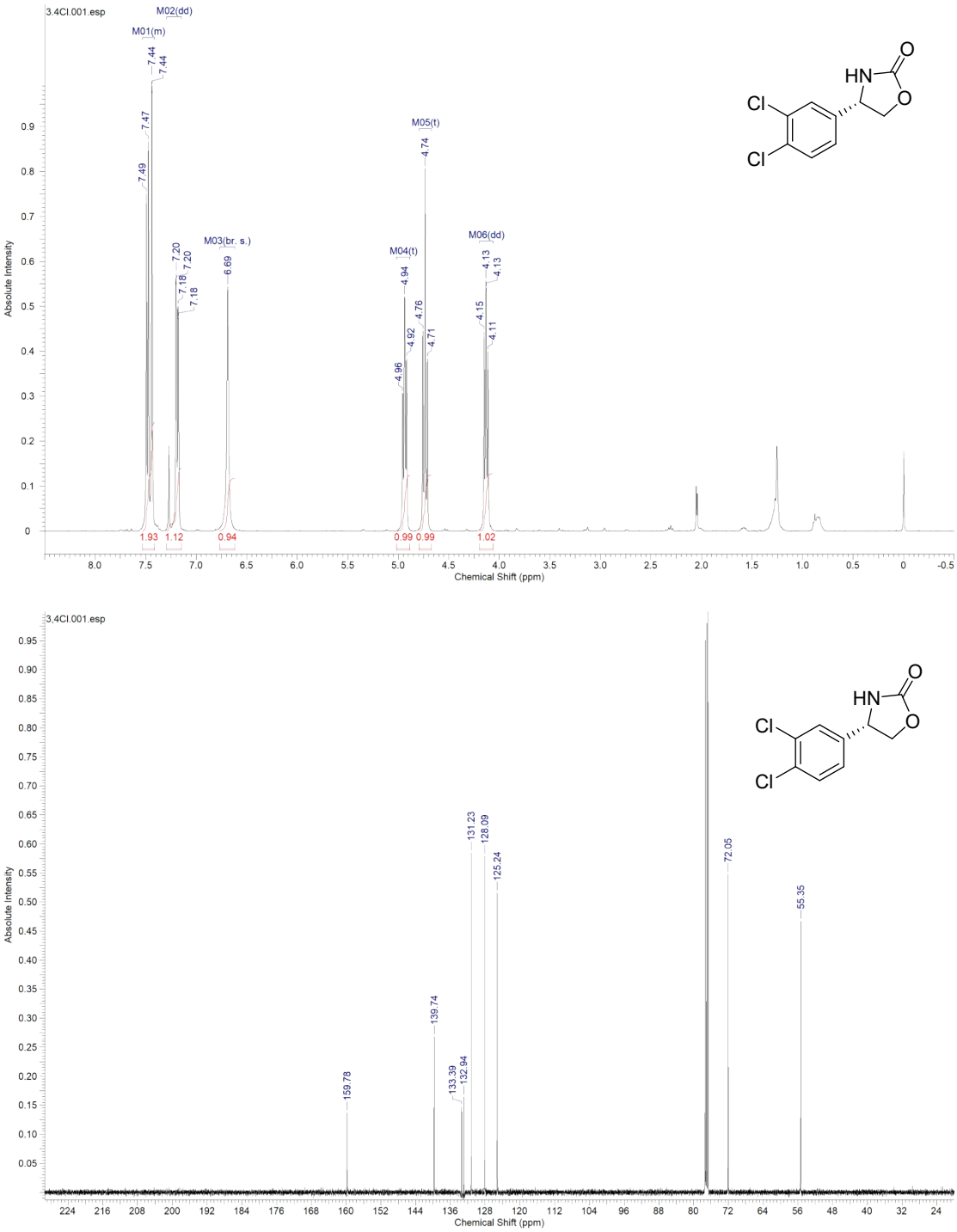

Fig. S42 NMR spectra copies of (*S*)-4-(3,4-dichlorophenyl)oxazolidin-2-one (**2l**).

References

(1) O. Mazimba, R. R. Majinda and I. B. Masesane, *B. Chem. Soc. Ethiopia.*, 2011, **25**, 299-304.

(2) (2) F. L. Li, Y. Y. Qiu, Y. C. Zheng, F. F. Chen, X. D. Kong, J. H. Xu and H. L. Yu, *Adv. Synth. Catal.*, 2020, **362**, 4699-4706.

(3) C. H. Zhou, X. Chen, T. Lv, X. Han, J. H. Feng, W. D. Liu, Q. Q. Wu and D. M. Zhu, *ACS. Catal.*, 2023, **13**, 4768-4777.

(4) N. Wan, J. Tian, X. Zhou, H. Wang, B. Cui, W. Han and Y. Chen, *Adv. Synth. Catal.*, 2019, **361**, 4651-4655.